NIMS Documentation

Release 3.1.0

Mercier D.

Sep 05, 2018

Contents

The NIMS toolbox has been developed to plot and to analyze (nano)indentation data (obtained with conical indenters) for bulk material or multilayer sample.

With this Matlab toolbox, it is possible to :

- plot and correct nanoindentation dataset with standard deviation ;
- calculate the coefficient of the power law fit of the load-displacement curve ;
- **calculate the energy of the loading (area below the load-displacement curve) ;**
  - plot of the stiffness and the load/stiffness^2 evolution;
- calculate the Young's modulus and hardness of bulk materials ;
- calculate the Young's modulus and hardness of thin films on a substrate (for a bilayer or a multilayer sample (until 3 layers on a substrate)) ;
- generate Python script of axisymmetrical FEM model for use in ABAQUS (cono-spherical indentation of multilayer sample).

Source code is hosted at Github.

Download source code as a .zip file.

Download the documentation as a pdf file.

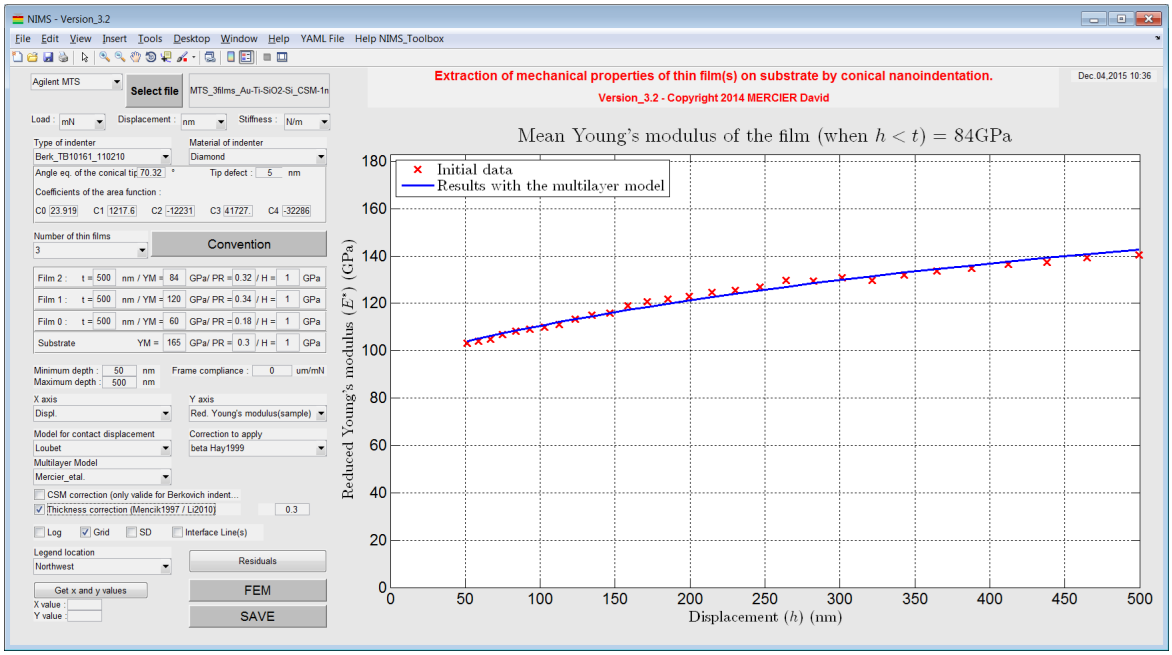

Figure 1: *Screenshot of the main window of the NIMS toolbox.*

CHAPTER 1

Contents

1.1 Getting started

First of all, download the source code of the Matlab toolbox.

Source code is hosted at Github.

To have more details about the use of the toolbox, please have a look to :

```
Getting_started.txt
```

1.1.1 How to use the GUI for indentation data analysis ?

First of all a GUI is a Graphical User Interface.

- Create or update your personal YAML config. file stored in the YAML folder

See here how to create / modify your YAML file...

- Run the following Matlab script and answer 'y' or 'yes' to add path to the Matlab search paths :

```
path_management.m
```

- Then, run the following Matlab script :

```
demo.m
```

- The following window opens:
- Import your (nano)indentation results, by clicking on the button 'Select file'. Click here to have more details about valid format of data.
- A load-displacement curve is plotted (with a power law fit). The loading work is also given in the title of the plot.
- It is possible to plot the stiffness (raw data) without setting the GUI for Young's modulus calculation.

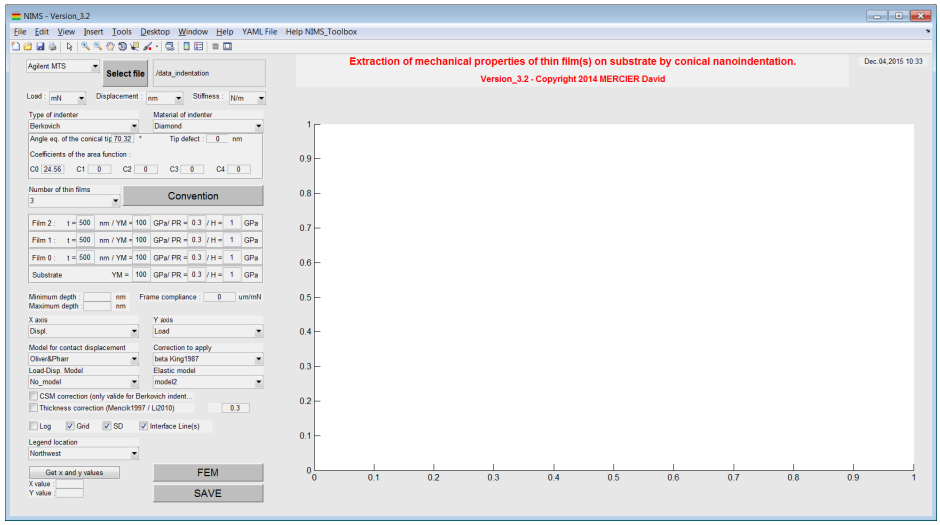

Figure 1.1: *Screenshot of the main window of the NIMS toolbox.*

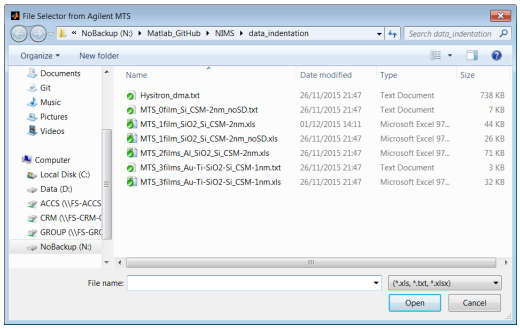

Figure 1.2: *File selector.*

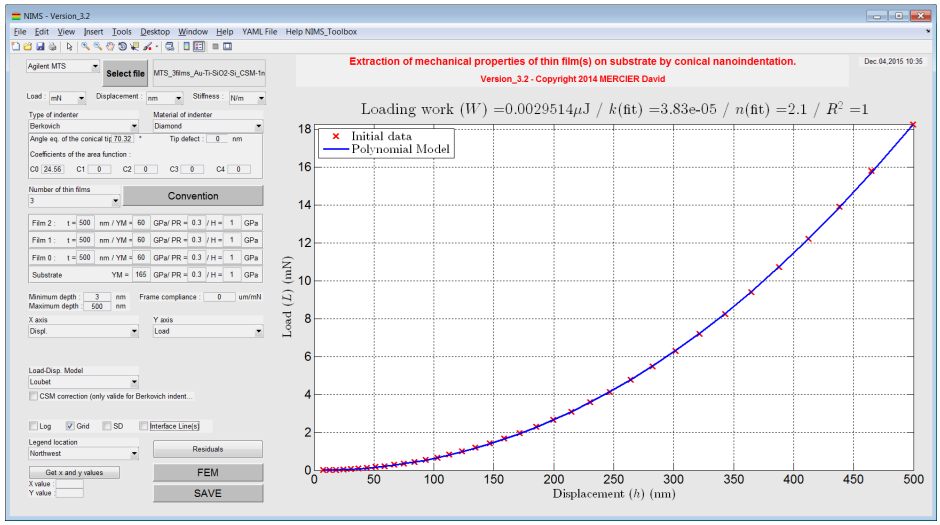

Figure 1.3: *Plot of the load-displacement curve after loading of data.*

- Choose and set (if needed) the indenter used to obtain (nano)indentation data.
- Select the lowest and the highest depth values (optional).
- Set the CSM correction (Berkovich indenter only !) (optional).
- Set the number of layers of your sample (0 = only bulk material, 1/2/3 = 1 to 3 thin layers on a substrate) (see Figure 1.4).

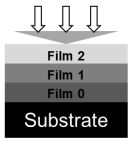

Figure 1.4: *Convention use to define multilayer specimen.*

- Set the thickness, the Poisson's coefficient and the Young's modulus to each layer.
- Select the model to use for the contact displacement calculation and select the correction to apply.
- Select 'Red. Young's modulus(film+sub)' or 'Red. Young's modulus(film)' in order to plot the evolution of the reduced Young's modulus (raw calculation) of the sample vs. the evolution of the reduced Young's modulus (modeled) of the sample and/or of the thin film.
- Select the analytical bilayer or the multilayer model to use for the modelling of the reduced Young's modulus of the top thin film.
- Press the button 'SAVE' and a YAML results file and a picture of the figure (.png format) are created and stored in the following folder.
- Press the button 'FEM' and generate a Python script to model nanoindentation of multilayer sample based on parameters used in the GUI for ABAQUS.

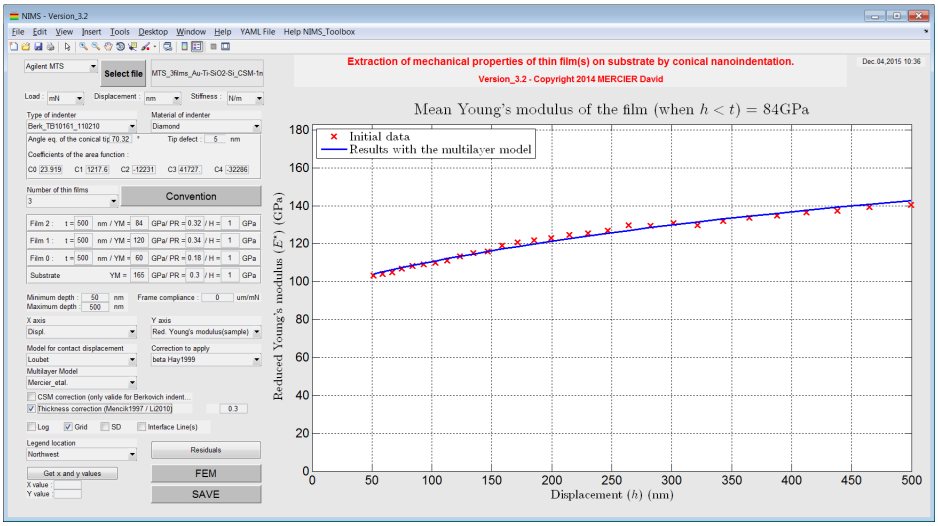

Figure 1.5: *Plot of the evolution of the Young's modulus of the sample with the elastic multilayer model in function of the indentation depth.*

1.1.2 Links

- Guidata on Matlab website.

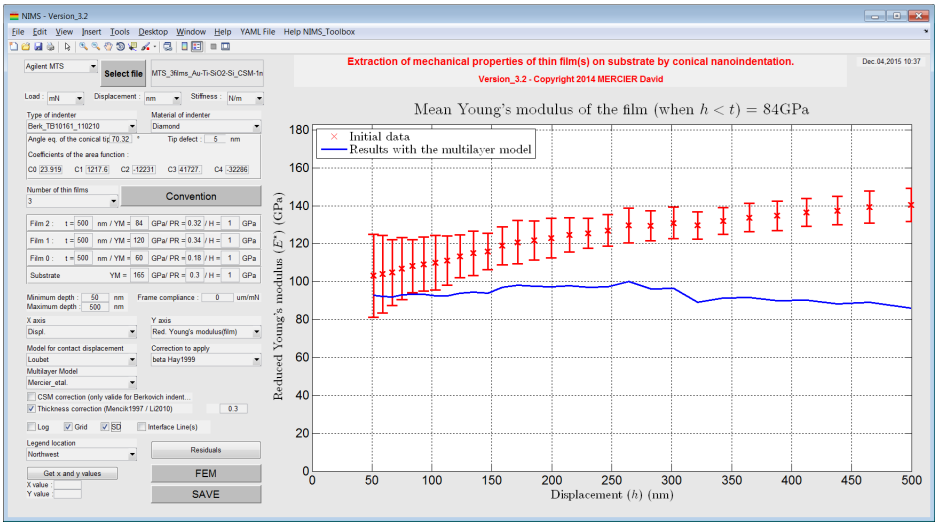

Figure 1.6: *Plot of the evolution of the Young's modulus of the film with the elastic multilayer model in function of the indentation depth.*

- Matlab GUI.
- Coding GUI behavior.

1.2 Configuration

1.2.1 What is a YAML File ?

"YAML is a human friendly data serialization standard for all programming languages."

Visit the YAML website for more informations.

Visit the YAML code for Matlab.

You have to update the YAML configuration files in order to use correctly Matlab toolbox.

1.2.2 The YAML configuration files

Three YAML configuration files are used in the Matlab toolbox :

- indenters_config.yaml provides indenter's properties (geometry and material).
- data_config.yaml provides a path on your computer to select easily your data.
- numerics_config.yaml provides numerical parameters used by the toolbox.

1.2.3 How to modify YAML configuration files ?

Please find the 3 YAML configuration files in the YAML folder.

indenters_config.yaml can be used to change indenter's properties :

- Write your Indenter_ID(s) (e.g. : Conical indenter, Berk_TB10161_091208, . . .);

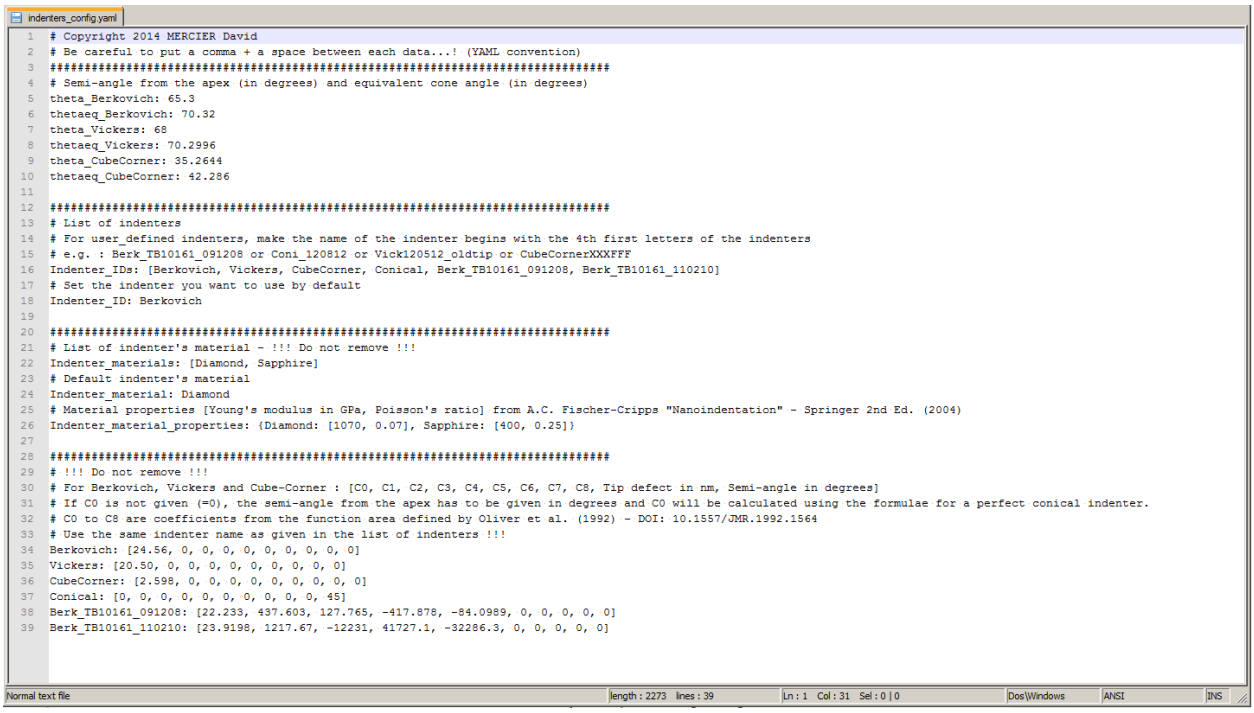

Figure 1.7: *Screenshot of the YAML configuration file used for indenter's properties.*

- Write indenter's properties (e.g. : Berk_TB10161_091208: [22.233, 437.603, 127.765, -417.878, -84.0989, 0]);

Warning:

- For user-defined indenters, make the name of the indenter begins with the 4th first letters of the indenter name (e.g.: 'Berk_130214' for 'Berkovich').
- Do not remove standard indenters and standard materials !

data_config.yaml can be used to set the default absolute path for the folder where you store your indentation data.

numerics_config.yaml can be used to change the numerical parameters used by the toolbox from their standard values.

Warning:

- Be careful to put a comma + a space between each data...! (YAML convention)
- Use # in the beginning of the line to add comments.

It is also possible to edit and to load the different YAML configuration files, via the customized menu of the GUI.

Note: To open and to modify these YAML files, you can directly use Matlab or any code editor (e.g. : Notepad++).

1.3 Models for bulk material

The nanoindentation (or instrumented or depth sensing indentation) is a variety of indentation hardness tests applied to small volumes. During nanoindentation, an indenter is brought into contact with a sample and mechanically loaded.

The following parts give a short overview of models existing in the literature used for the extraction of mechanical properties of homogeneous bulk materials from indentation experiments with conical (sharp) indenters.

Please look at the ISO standard (ISO 14577 - 1 to 3), to perform nanoindentation tests on bulk material.

- ISO 14577 - 1 , "Metallic materials – Instrumented indentation test for hardness and materials parameters – Part 1: Test method", (2002).
- ISO 14577 - 2 , "Metallic materials – Instrumented indentation test for hardness and materials parameters – Part 2: Verification and calibration of testing machines", (2002).
- ISO 14577 - 3 , "Metallic materials – Instrumented indentation test for hardness and materials parameters – Part 3: Calibration of reference blocks", (2002).

Some authors overviewed/reviewed already the nanoindentation technique :

- Li X. and Bhushan B., "A review of nanoindentation continuous stiffness measurement technique and its applications." (2002).
- VanLandingham M.R., "Review of Instrumented Indentation" (2003).
- Oliver W.C. and Pharr G.M., "Measurement of hardness and elastic modulus by instrumented indentation: Advances in understanding and refinements to methodology" (2004).
- Fischer-Cripps A.C., "Critical review of analysis and interpretation of nanoindentation test data" (2006).
- Fischer-Cripps A.C., "Nanoindentation" Springer 3rd Ed. (2011).
- Lucca D.A. et al., "Nanoindentation: Measuring methods and applications" (2012).
- Němeček J., "Nanoindentation in Material Science" (2012).
- Michailidis N. et al., "Nanoindentation" (2014).

1.3.1 Nanoindentation tests on bulk material

Conical indenters

The geometric properties of conical indenters are well described in[9].

[9] Fischer-Cripps A.C., "Nanoindentation" Springer 3rd Ed. (2011).

Table 1.1: **Geometric properties of conical indenters.**

Indenter	Berkovich	Vickers	Cube-Corner	Conical
Shape	3-sided pyramid	4-sided pyramid	3-sided pyramid	Conical (angle ψ)
Semi-angle from the apex	65.3°	68°	35.2644°	–
Equivalent cone angle	70.32°	70.2996°	42.28°	ψ
Projected Area	$24.56h^2$	$24.504h^2$	$2.5981h^2$	$\pi {a_c}^2$
Volume-depth relation	$8.1873h^3$	$8.1681h^3$	$0.8657h^3$	–
Projected area/face area	0.908	0.927	0.5774	–
Contact radius	–	–	–	$htan\psi$

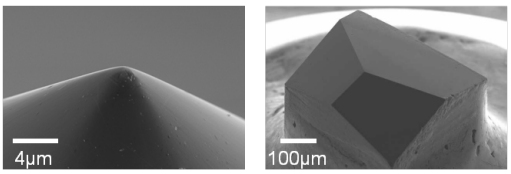

Figure 1.8: *a) Conical indenter (45°) and b) Berkovich indenter.*

These indenters have self-similar geometries which implies a constant strain and similarity of the stress fields.

Note: Indenters are mainly in diamond. Diamond has a Young's modulus of 1070GPa and a Poisson's ratio of 0.07[9].

Load-Displacement curves

In this first part, only quasistatic (or monotonic) nanoindentation is considered, when a load is applied and removed to a sample. Parameters such as contact load F_c (in N) and depth of penetration (displacement) h_0 (in m) are continuously recorded at a rapid rate (normally 10Hz) during loading and unloading steps of the indentation test. Usually, the depth resolution is around the nm-level and the load resolution is around nN-level.

Initial penetration

The first correction step in nanoindentation testing is the determination of the initial contact point between the indenter and the sample[10].

Usually, the point of contact is determined from the load-displacement curve, when a sharp rise in the force signal is observed. Then, initial penetration h_i is estimated by extrapolating the recorded load–displacement data back to zero load.

$$h = h_0 + h_i \tag{1.1}$$

[10] Fischer-Cripps A.C., "Critical review of analysis and interpretation of nanoindentation test data" (2006).

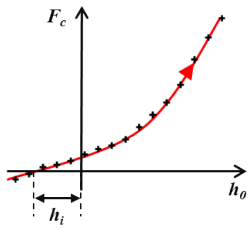

Figure 1.9: *Schematic of the estimation of initial point.*

With h the corrected penetration and h_0 the recorded penetration.

A schematic of the load-displacement curve obtained from nanoindentation experiment after this first correction is given Figure 1.10.

The evolution of this curve depends on material properties of the sample and the indenter, and of the indenter's geometry.

The tangent (or the slope) of the part of the unloading curve at the maximum load gives access to the contact stiffness S (in N/m):

$$S = \frac{dF_c}{dh} \tag{1.2}$$

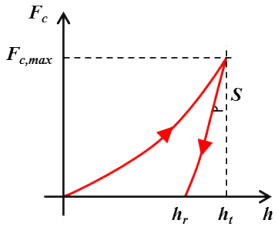

Figure 1.10: *Schematic of indentation load-displacement curve.*

With h_t the total penetration corrected of the frame compliance and h_r the residual indentation depth after unloading.

It is worth to mention that for quasistatic nanoindentation, the contact stiffness is a unique value obtained at the maximum load and at the maximum displacement. Nevertheless, it is possible to apply a multiple-point unload method, and then determine the contact stiffness for many indentation depths, in function of the number of points defined by the user (see Figure 1.11)[9].

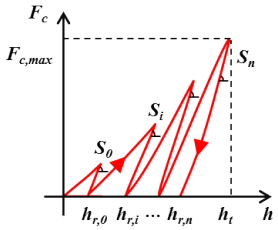

Figure 1.11: *Schematic of indentation load-displacement curve with the multiple point unload method (here n points).*

Frame compliance

Before any analysis, it is important to correct raw data of the effect of the frame compliance. The frame compliance is defined by the deflections of the load frame instead of displacement into the studied material. This frame compliance C_f (in m/N) contributes to the measured indentation depth and to the contact stiffness[10].

$$h_\mathrm{t} = h - F_\mathrm{c} C_\mathrm{f} \tag{1.3}$$

$$S = \left(\frac{dh}{dF_\mathrm{c}} - C_\mathrm{f} \right)^{-1} \tag{1.4}$$

To determine the frame compliance, it is required to plot $\frac{dh}{dF_\mathrm{c}}$ vs. the corrected total depth $(1/h_\mathrm{t})$ or the corrected plastic depth $(1/h_\mathrm{c})$ (see the following part "Indentation contact topography" for the definition of the plastic depth)[8] and[10]. Then, a linear fit of this curve gives an intercept with the ordinate axis which is the frame compliance (see Figure 1.12).

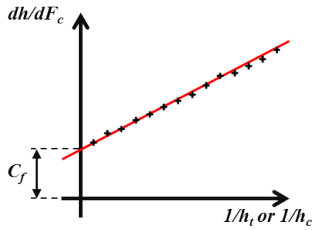

Figure 1.12: *Schematic of the plot to determine the frame compliance.*

It is advised to perform indentation tests on a variety of bulk standard specimens (fused silica, silicon and sapphire provide a very good range), in order to estimate better the frame compliance.

Moreover, when the sample flexes or has heterogeneities (free edges, interfaces between regions of different properties…), nanoindentation measurements are affected by the structural compliance C_s. Then, it is possible to correct experimental data of this artifact by following the experimental approach proposed by[19].

Loading

Loubet et al. founded a good fit to the loading part of the load-displacement curve with a power-law relationship of the form[25] :

$$F_\mathrm{c} = K h_\mathrm{t}^n \tag{1.5}$$

With K and n constants for a given material for a fixed indenter geometry.

It is possible to find in the litterature sometimes the following equation to fit the loading curve:

$$F_\mathrm{c} = K h_\mathrm{t}^n + C \tag{1.6}$$

With C a constant which is used to account a small preload prior indentation testing[31].

[8] Doerner M.F. and Nix W.D., "A method for interpreting the data from depth-sensing indentation instruments" (1986).
[19] Jakes J.E. et al., "Experimental method to account for structural compliance in nanoindentation measurements" (2008).
[25] Loubet J.L. et al., "Vickers indentation curves of elastoplastic materials." (1986).
[31] Morash K.R. and Bahr D.F., "An energy method to analyze through thickness thin film fracture during indentation." (2007).

Using the load-displacement curves analysis performed by Loubet et al., Hainsworth et al. proposed the following relationship to describe loading curves[16] :

$$F_c = K h_t^2 \tag{1.7}$$

With K a constant function of material properties (Young's modulus and hardness) and the indenter.

In the same time, Giannakopoulos and Larsson established parabolic relationships between the load and the indentation depth, for purely elastic indentation of bulk materials with ideally Berkovich indenter (1.8)[22] and Vickers indenter (1.9)[12], by numerical studies.

$$F_c = 2.1891 \left(1 - 0.21\nu - 0.01\nu^2 - 0.41\nu^3\right) \frac{E}{1-\nu^2} h_t^2 \tag{1.8}$$

$$F_c = 2.0746 \left(1 - 0.1655\nu - 0.1737\nu^2 - 0.1862\nu^3\right) \frac{E}{1-\nu^2} h_t^2 \tag{1.9}$$

With ν the Poisson's ratio and E the Young's modulus of the indented material.

Finally, it is first important to cite the work of Malzbender et al., who developped the relationship between the load and the indentation depth for elastoplastic materials, based on the knowledge of the Young's modulus and the hardness values of the material[29]. Then, It is worth to mention the model of Oyen et al., who described sharp indentation behavior of time-dependent materials[34].

Unloading

Pharr and Bolshakov founded that unloading curves were well described by the following power-law relationship[36] :

$$F_c = \alpha_u \left(h_t - h_r\right)^m \tag{1.10}$$

Where h_r is the final displacement after complete unloading, and α_u and m are material constants. Many experiments performed by Pharr and Bolshakov leaded to an average value for m close to 1.5 for the Berkovich indenter.

Loading rate

The mechanical response of a material is function of the imposed indentation strain rate $\dot{\epsilon}$ (in s^{-1})[28]. Thus, it is meaningful to perform indentation tests with a constant indentation strain rate.

$$\dot{\epsilon} = \frac{\dot{h}}{h} = \frac{1}{2}\frac{\dot{F_c}}{F_c} \tag{1.11}$$

[16] Hainsworth S.V. et al., "Analysis of nanoindentation load-displacement loading curves." (1996).
[22] Larsson P.-L. et al., "Analysis of Berkovich indentation" (1996).
[12] Giannakopoulos A.E. et al., "Analysis of Vickers indentation" (1994).
[29] Malzbender J. and de With G., "Indentation load–displacement curve, plastic deformation, and energy." (2002).
[34] Oyen M.L. et al., "Load–displacement behavior during sharp indentation of viscous–elastic–plastic materials" (2003).
[36] Pharr G.M. and Bolshakov A., "Understanding nanoindentation unloading curves." (2002).
[28] Lucas B.N. et al., "Time Dependent Deformation During Indentation Testing." (1996).

Indentation contact topography

The indentation total depth is rarely equal to the indentation contact depth. Two kind of topography can occur:

- the pile-up (indentation contact depth > indentation total depth) (see Figure 1.13 a and Figure 1.14);
- the sink-in (indentation contact depth < indentation total depth) (see Figure 1.13 b).

The flow of material below the indenter is function of mechanical properties of the material.

Pile-up occurs when work-hardening coefficient is low (< 0.3) or if the ratio yield stress over Young's modulus is less than 1[4], [5]and[7].

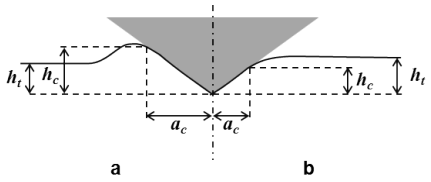

Figure 1.13: *Schematic of indentation contact topography : a) "pile-up" and b) "sink-in".*

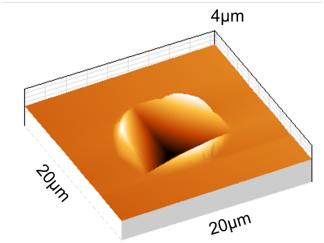

Figure 1.14: *Residual topography of a Berkovich indent in PVD Gold thin film (500nm thick) with "pile-up" surrounding the indent, measured by atomic force microscopy.*

Three main models defining the depth of contact h_c were developed to take into account this indentation contact topography.

Model of Doerner and Nix[8] :

$$h_c = h_t - \frac{F_c}{S} \tag{1.12}$$

Model of Oliver and Pharr[32],[36] and[33] in case of sink-in:

$$h_c = h_t - \epsilon\frac{F_c}{S} \tag{1.13}$$

[4] Bolshakov A. and Pharr G.M., "Influences of pile-up on the measurement of mechanical properties by load and depth sensing indentation techniques." (1998)

[5] Cheng Y.T. and Cheng C.M. ,"Effects of 'sinking in' and 'piling up' on estimating the contact area under load in indentation." (1998)

[7] Cheng Y.T. and Cheng C.M., "Scaling, dimensional analysis, and indentation measurements." (2004)

[32] Oliver W.C. and Pharr G.M., "An improved technique for determining hardness and elastic modulus using load and displacement sensing indentation experiments" (1992).

[33] Oliver W.C. and Pharr G.M., "Measurement of hardness and elastic modulus by instrumented indentation: Advances in understanding and refinements to methodology" (2004).

Where ϵ is a function of the indenter's geometry (0.72 for conical indenter, 0.75 for paraboloids of revolution and 1 for a flat cylindrical punch). An expression of ϵ in function of the power law exponent m of the unloading curve fit has been proposed by Pharr et Bolshakov[36] :

$$\epsilon = m\left(1 - \frac{2\Gamma\left(\frac{m}{2(m-1)}\right)}{\sqrt{\pi}\Gamma\left(\frac{1}{2(m-1)}(m-1)\right)}\right)$$

With Γ a Matlab function which interpolates the factorial function : gamma.

Find here the Matlab function to plot the ϵ function : epsilon_oliver_pharr.m.

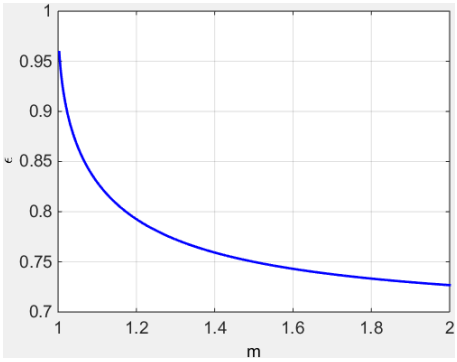

Figure 1.15: *Evolution of epsilon in function of the power law exponent m of the unloading curve.*

0.72 should be most applicable for a Berkovich indenter, which is more like a cone than a paraboloid of revolution. But, Oliver and Pharr concluded after a large number of experiments that the best value for the Berkovich indenter is 0.75.

More recently, Merle et al. have found experimentally with indentation test in fused silica, a value of 0.76 for ϵ, which is in a good agreement with the literature for a paraboloid of revolution[30].

Model of Loubet et al.[18],[1] in case of pile-up:

$$h_c = \alpha\left(h_t - \frac{F_c}{S} + h_0\right) \tag{1.14}$$

Where α is a constant function of the indented material (usually around 1.2) and the tip-defect h_0.

Knowing the depth of contact, it is possible to determine the area of contact A_c (in m^2) for a perfect conical indenter (with a semi-angle from the apex θ):

$$A_c = \pi h_c^2 tan^2\left(\theta\right) \tag{1.15}$$

But, because conical indenters present imperfections and Berkovich or Vickers indenters are not perfectly conical, a general formulae of the contact area has been established by Oliver and Pharr[32],[33] :

[30] Merle B. et al., "Experimental determination of the effective indenter shape and e-factor for nanoindentation by continuously measuring the unloading stiffness." (2012).

[18] Hochstetter G. et al., "Strain-rate effects on hardness of glassy polymers in the nanoscale range. Comparison between quasi-static and continuous stiffness measurements" (1999).

[1] Bec S. et al., "Improvements in the indentation method with a surface force apparatus" (2006).

$$A_c = C_0 h_c^2 + \sum_{n=1}^{8} C_n h_c^{1/2^{n-1}} \tag{1.16}$$

With the coefficients C_0 and C_n obtained by curve fitting procedures, from nanoindentation experiments in fused silica (amorphous and isotropic material).

For a perfect Berkovich indenter C_0 is equal to 24.56 and for a perfect Vickers indenter C_0 is equal to 24.504 (see Table 1.1).

The second term of the area function A_c describes a paraboloid of revolution, which approximates to a sphere at small penetration depths. A perfect sphere of radius R is defined by the first two terms with $C_0 = -\pi$ and $C_1 = 2\pi R$. The first two terms also describe a hyperboloid of revolution, a very reasonable shape for a tip-rounded cone or pyramid that approaches a fixed angle at large distances from the tip.

An equivalent contact radius a_c (in m) is also defined based on the area function.

$$a_c = \sqrt{\frac{A_c}{\pi}} \tag{1.17}$$

One other way to express the function area is that suggested by Loubet et al.[24], which describes a pyramid with a small flat region on its tip, the so-called tip defect (h_0). This geometry is described by the addition of a constant to the first two terms in (1.16).

Find here the Matlab function to calculate the contact depth, the function area and the contact radius: model_function_area.m.

Recently, in the paper of Yetna N'jock M. et al.[43], a criterion was proposed to forecast the behaviour during indentation experiments, following Giannakopoulos and Suresh methodology[13]. After analyzing either Vickers or Berkovich indentation tests on a wide range of materials, the following criterion is established Δ :

$$\Delta = \frac{h_r'}{h_t'} \tag{1.18}$$

With h_r' and h_t' residual contact depth and maximum depth after applying a compliance correction. Three preponderant deformation modes are distinguished :

- $\Delta = 0.83$ no deformation mode is preponderant;
- $\Delta < 0.83$ implies sink-in formation;
- $\Delta > 0.83$ implies pile-up formation.

Giannakopoulos and Suresh founded a critical value for a similar criterion about 0.875[13].

Dynamic nanoindentation

The dynamic indentation is when a small dynamic oscillation (usually 2nm of amplitude) with a given frequency (ω) (usually 45Hz) is imposed on the force (or displacement) signal. The amplitude of the displacement (or load) and the phase angle between the force and displacement signals (ϕ) are measured using a frequency-specific amplifier. This technique allows to calculate the elastic stiffness and so the elastic properties continuously during the loading of the indenter[32],[23]. This technique is named **Continuous Stiffness Measurement** (CSM) for Agilent - MTS nanoindenter

[24] Loubet J.L. et al., "Vickers Indentation Curves of Magnesium Oxide (MgO)." (1984).
[43] Yetna N'jock M. et al., "A criterion to identify sinking-in and piling-up in indentation of materials." (2015).
[13] Giannakopoulos A.E. and Suresh S., "Determination of elastoplastic properties by instrumented sharp indentation." (1999).
[23] Li X. and Bhushan B., "A review of nanoindentation continuous stiffness measurement technique and its applications." (2002).

and **Dynamic Mechanical Analysis** (DMA) (using the CMX control algorithms) for Hysitron nanoindenter.

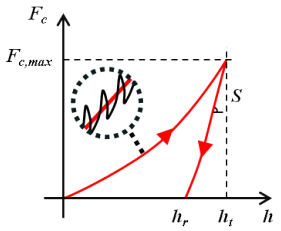

Figure 1.16: *Schematic of the dynamic loading cycle.*

$$S = \left[\frac{1}{\frac{F_c}{h_t}\cos\phi - (K_s - m\omega^2)} - \frac{1}{K_f} \right]^{-1} \tag{1.19}$$

$$C\omega = \frac{F_c}{h_t}\sin\phi - C_s\omega \tag{1.20}$$

With m the mass of the indenter column, C the harmonic contact damping in N.s/m, C_s the system damping coefficient in N.s/m, K_s the stiffness of the indenter support springs in N/m and K_f the stiffness of the load frame in N/m.

Values m, C_s, K_s and K_f are function of the equipment used and are determined during calibration process.

This solution allows to determine the material properties as a continuous function of the indentation depth, but Pharr et al. have highlighted the influence of displacement oscillation on the basic measured quantities[37]. According to the authors, *"the sources of the measurement error have their origin in the relative stiffness of the contact and its relation to the displacements that can be recovered during the unloading portion of the oscillation"*. Based on that, the authors proposed the following corrections to determine the actual load ($F_{c,act}$), the actual displacement ($h_{t,act}$) and the actual stiffness (S_{act}):

$$F_{c,act} = F_c + \frac{\Delta F_c}{2} = F_c + \sqrt{2}\Delta F_{c,rms} \tag{1.21}$$

$$h_{t,act} = h_t + \frac{\Delta h_t}{2} = h_t + \sqrt{2}\Delta h_{t,rms} \tag{1.22}$$

$$S_{act} = \frac{1}{\sqrt{2\pi}} \left(\frac{1}{K}\right)^{\frac{1}{m}} \left[1 - \left(1 - S\frac{2\sqrt{2}\Delta h_{t,rms}}{F_{c,max}} \right)^{\frac{1}{m}} \right] \frac{F_{c,max}}{\Delta h_{t,rms}} \tag{1.23}$$

With K and m constants determined from unloading curves. These constants are related by the following equation :

$$K = \left(\frac{2}{m\sqrt{\pi}} \right)^m \tag{1.24}$$

Pharr and Bolshakov founded a value of 1.380 for m after many Berkovich indentation tests on a variety of materials[36]. Thus, a value of 0.757 is used for the constant K, using (1.24).

Find here the Matlab function to calculate the corrections to apply on depth, load and stiffness during dynamic nanoindentation: CSM_correction.m.

Find here the Matlab function to calculate the constant K in function of m: unload_k_m.m.

[37] Pharr G.M. et al., "Critical issues in making small-depth mechanical property measurements by nanoindentation with continuous stiffness measurement" (2009).

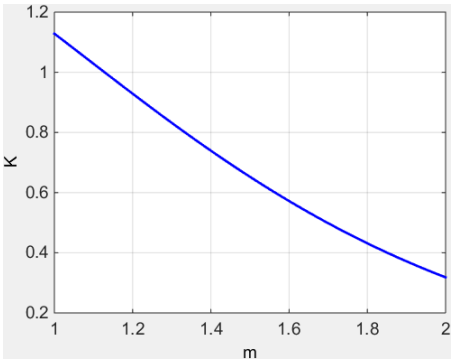

Figure 1.17: *Evolution of K in function of m.*

1.3.2 Extraction of elastic properties

Elastic properties of bulk material

Bulychev et al.[3] and Shorshorov M. K. et al.[39] were the first to determine the reduced Young's modulus of a material with the relationships established by Love[26], Galin[11] and Sneddon[38], between the applied load and the displacement during an indentation test of an elastic material.

They proposed to expressed the reduced Young's modulus E^* (in GPa $=$ N/m^2) in function of the contact area and the contact stiffness :

$$E^* = \frac{1}{2}\sqrt{\frac{\pi}{A}}S \tag{1.25}$$

Then, Oliver and Pharr[35],[32] democratized this formulae after introducing a correction factor identified by King[21] :

$$E^* = \frac{1}{2\beta}\sqrt{\frac{\pi}{A}}S \tag{1.26}$$

With β a geometrical correction factor equal to :

- 1 for circular indenters (e.g.: conical and spherical indenter);
- 1.034 for three-sided pyramid indenters (e.g.: Berkovich indenter);
- 1.012 for four-sided pyramid indenters (e.g.: Vickers indenter).

Woirgard has demonstrated analytically that the exact value of β for the perfectly sharp Berkovich indenter should be 1.062[41].

[3] Bulychev S.I. et al., "Determining Young's modulus from the indentor penetration diagram.", Zavod. Lab., 1973, 39, pp. 1137-1142.
[39] Shorshorov M.K. et al., Sov. Phys. Dokl., 1982, 26.
[26] Love A.E.H., "Boussinesq's problem for a rigid cone." (1939).
[11] Galin L.A., "Spatial contact problems of the theory of elasticity for punches of circular shape in planar projection.", J. Appl. Math. Mech. (PMM) (1946), 10, pp. 425-448.
[38] Sneddon I.N., "Boussinesqs problem for a rigid cone." (1948).
[35] Pharr G.M. et al., "On the generality of the relationship among contact stiffness, contact area, and elastic modulus during indentation." (1992).
[21] King R.B., "Elastic analysis of some punch problems for a layered medium" (1987).
[41] Troyon M. and Lafaye S., "About the importance of introducing a correction factor in the Sneddon relationship for nanoindentation measurements" (2002).

Some authors proposed another correction factor function of the angle of the conical indenter and the Poisson's ratio of the indented material[17] and[40]. For a conical indenter with an half-angle of $\gamma \leq 60°$ (e.g.: Cube-Corner indenter), the analytical approximation is :

$$\beta = 1 + \frac{(1-2\nu)}{4\,(1-\nu)\,tan\gamma} \tag{1.27}$$

For a conical indenter with larger half-angle (e.g.: Berkovich indenter), the analytical approximation is :

$$\beta = \pi \frac{\pi/4 + 0.1548 cot\gamma \frac{1-2\nu}{4(1-\nu)}}{\left[\pi/2 - 0.8311 cot\gamma \frac{1-2\nu}{4(1-\nu)}\right]^2} \tag{1.28}$$

With ν the Poisson's ratio of the indented material.

Find here the Matlab function to plot the β function of Hay et al.: beta_hay.m.

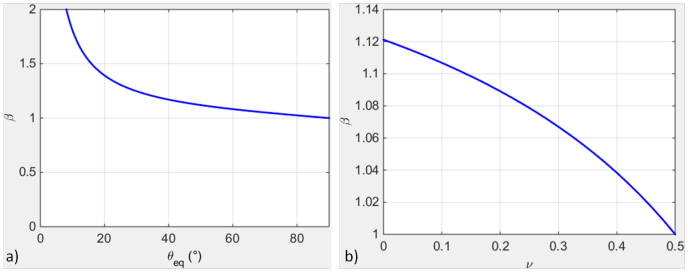

Figure 1.18: *Plots of beta Hay : a) in function of the half-angle of the conical indenter (for a Poisson's ratio of 0.3), and b) in function of the Poisson's ratio for a Berkovich indenter.*

Knowing the material properties of the indenter, it is possible to calculate the reduced Young's modulus $E^{'}$ (in GPa $=$ N/m^2) of the indented material.

$$\frac{1}{E'} = \frac{1}{E^*} - \frac{1}{E'_{\mathrm{i}}} \tag{1.29}$$

$$E = E^{'}\left(1-\nu^2\right) \tag{1.30}$$

$$E'_{\mathrm{i}} = \frac{E_{\mathrm{i}}}{(1-\nu_{\mathrm{i}}^2)} \tag{1.31}$$

With ν the Poisson's ratio of the indented material and ν_{i} the Poisson's ratio of the material of the indenter.

Note: This method used to analyze indentation data is based on equations valid for isotropic homogeneous elastic solids.

Find here the Matlab function to calculate the Young's modulus: model_elastic.m.

If dynamic nanoindentation is performed, a loss modulus $E^{'*}$ (in GPa $=$ N/m^2) can be defined by the following equation :

[17] Hay J.C. et al., "A critical examination of the fundamental relations used in the analysis of nanoindentation data." (1999).
[40] Strader J.H. et al., "An experimental evaluation of the constant b relating the contact stiffness to the contact area in nanoindentation." (2006).

$$E'^{*} = \frac{C\omega}{2}\sqrt{\frac{\pi}{A}} \tag{1.32}$$

Find here the Matlab function to calculate the loss modulus: loss_modulus.m.

1.3.3 Extraction of plastic properties

The hardness H (in GPa $=$ N/m^2) of the material is defined according to Oliver and Pharr[32], by the following expression :

$$H = \frac{F_{\mathrm{c,max}}}{A_{\mathrm{c}}} \tag{1.33}$$

Find here the Matlab function to calculate the hardness: model_hardness.m.

1.3.4 Energy approach

Another way to access indentation data is the use of the energy W_{tot} (in J $=$ N/m) dissipated during the indentation. The elastic W_{e} and plastic W_{p} energies are respectively based on the integrals of the loading and unloading curves (see Figure 1.19)[6] and[29].

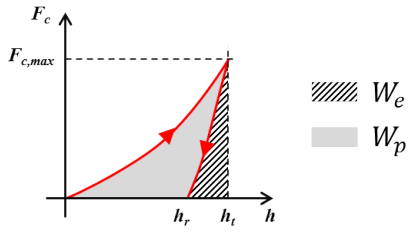

Figure 1.19: *Schematic representation of indentation load–displacement curves with definition of different works of indentation.*

$$W_{\mathrm{tot}} = \int_0^{h_{\mathrm{t}}} F_{\mathrm{c}}\,(dh) \tag{1.34}$$

$$W_{\mathrm{e}} = \int_{h_{\mathrm{r}}}^{h_{\mathrm{t}}} F_{\mathrm{c}}\,(dh) \tag{1.35}$$

$$W_{\mathrm{p}} = W_{\mathrm{tot}} - W_{\mathrm{e}} \tag{1.36}$$

The “trapz” Matlab function is used to calculate the area below the load-displacement curve: trapz.m.

1.3.5 Methodology to extract properties without the function area

The ratio of the irreversible work $W_{\mathrm{tot}} - W_{\mathrm{e}}$ to the total work W_{tot}, appears to be a unique function of the Young’s modulus and the hardness of the material, independent of the work-hardening behavior[6].

[6] Cheng Y.T. and Cheng C.M. ,”Relationships between hardness, elastic modulus, and the work of indentation.” (1998)

$$\frac{W_{\text{tot}} - W_{\text{e}}}{W_{\text{tot}}} = 1 - 5\frac{H}{E^*} \tag{1.37}$$

Then, combining the expression of the reduced Young's modulus (1.26) with the expression of the hardness (1.33), leads to the following equation[20] and[33]:

$$\beta\frac{4}{\pi}\frac{F_{\text{c,max}}}{S^2} = \frac{H}{E^*} \tag{1.38}$$

The β is initially not present in the equation given by[20].

These two last equations represent two independent relations that can be solved for H and E^* in a manner that does not directly involve the contact area.

The equation (1.38) is used as well to determine coefficients of the function area (1.16). Based on the assumption that the hardness and the Young's modulus remain constant during indentation test in fused silica (isotropic material), the evolution of the ratio $\frac{F_{\text{c,max}}}{S^2}$ should stay constant as well in function of the indentation depth.

More recently, Guillonneau et al. proposed a model to extract mechanical properties without using the indentation depth[14] and[15]. The method is based on the detection of the second harmonic for dynamic indentation testing. This model is interesting especially for penetration depths in the range of 25 to 100nm, where the uncertainties related to the displacement measurement disturb a lot.

1.3.6 References

1.4 Models for thin films

The following parts give a short overview of models existing in the literature used for the extraction of mechanical properties of thin films deposited on a substrate from indentation experiments with conical indenters.

Before everything, it is is worth to mention the work performed by Jennett N.M. and Bushby A.J.[24], about nanoindentation test on coatings, during the European project INDICOAT (SMT4-CT98-2249).

Progress from this project help in the development of the ISO standard (ISO 14577 - 1-4). The ISO 14577 - 4 is dedicated to nanoindentation on coatings.

- ISO 14577 - 1 , "Metallic materials – Instrumented indentation test for hardness and materials parameters – Part 1: Test method", (2002).
- ISO 14577 - 2 , "Metallic materials – Instrumented indentation test for hardness and materials parameters – Part 2: Verification and calibration of testing machines", (2002).
- ISO 14577 - 3 , "Metallic materials – Instrumented indentation test for hardness and materials parameters – Part 3: Calibration of reference blocks", (2002).
- ISO 14577 - 4 , "Metallic materials – Instrumented indentation test for hardness and materials parameters – Part 4: Test method for metallic and non-metallic coatings", (2007).

Some authors overviewed/reviewed already the nanoindentation technique applied to coatings :

[20] Joslin D.L. and Oliver W.C., "A new method for analyzing data from continuous depth-sensing microindentation tests" (1990).
[14] Guillonneau G. et al.,"Extraction of mechanical properties with second harmonic detection for dynamic nanoindentation testing." (2012).
[15] Guillonneau G. et al.,"Determination of mechanical properties by nanoindentation independently of indentation depth measurement." (2012).
[24] Jennett N. M. and Bushby A. J., "Adaptive Protocol for Robust Estimates of Coatings Properties by Nanoindentation" (2001).

- Pharr G.M. and Oliver W.C., "Measurement of Thin Film Mechanical Properties Using Nanoindentation" (1992).
- Menčík J. et al., "Determination of elastic modulus of thin layers using nanoindentation" (1997).
- Nix W.D., "Elastic and plastic properties of thin films on substrates: nanoindentation techniques" (1997).
- Van Vliet K.J. and Gouldstone A., "Mechanical Properties of Thin Films Quantified Via Instrumented Indentation" (2001).
- Šimůnková Š., "Mechanical properties of thin film–substrate systems" (2003).
- Bull S.J., "Nanoindentation of coatings" (2005).
- Fischer-Cripps, A.C., "Nanoindentation 3rd Ed." (2011)

1.4.1 Nanoindentation tests on thin films

Composite reduced Young's modulus and composite hardness

For indentation test on a coated specimen or on a multilayer sample (e.g.: thin films deposited on a substrate), the evolution of the Young's modulus or the hardness calculated with models used for bulk materials, is function of the material properties and the thickness t (in m) of each underlying film (substrate included), and the properties and the geometry of the indenter.

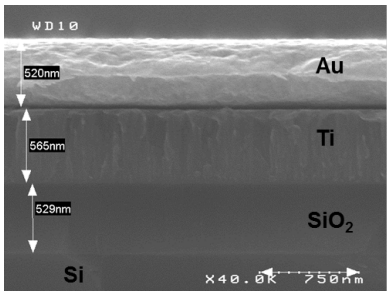

Figure 1.20: *SEM cross-sectional observation of a multilayer sample.*

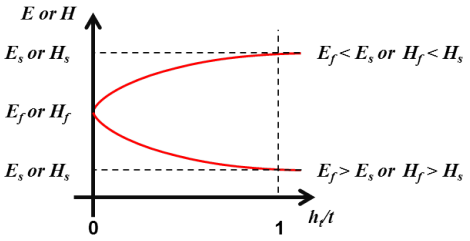

Figure 1.21: *Typical evolution of Young's modulus and hardness for a coated specimen in function of the normalized indentation depth.*

Thus, the composite reduced Young's modulus $E^{'}$ and the composite hardness H calculated with the models used for bulk materials, can generally be expressed as a combination of respectively the reduced Young's moduli $(E_{\mathrm{f}}^{'})$ or the hardness (H_{f}) of each underlayer and respectively the reduced Young's modulus $(E_{\mathrm{s}}^{'})$ or the hardness (H_{s}) of the substrate. The reduced Young's moduli and the hardness are in GPa.

$$E^{'} = f(E^{'}_{\mathrm{f},i\rightarrow N}, t_{i\rightarrow N}, E^{'}_{\mathrm{s}}) \tag{1.39}$$

$$H = f(H_{\mathrm{f},i\rightarrow N}, t_{i\rightarrow N}, H_{\mathrm{s}}) \tag{1.40}$$

With i the indice of the layer and N the total number of layers.

Indentation contact topography

For nanoindentation tests on thin films, the contact topography is function of both thin film and substrate properties.

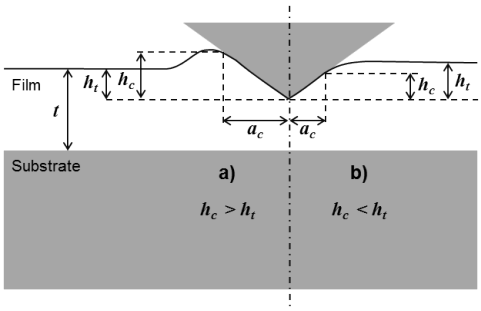

Figure 1.22: *Schematic depiction of a) "pile-up" and b) "sink-in" observed during thin film indentation.*

The Figure 1.22 a ("pile-up") is typical of the case of a soft film on a hard substrate and the Figure 1.22 b ("sink-in") of a hard film on a soft substrate[9]. The pile-up can be emphasized in case ot thin films, because of the material confinement by the substrate. To determine the depth of contact, the same models described for bulk material indentation are used.

Corrections to apply for thin film indentation

During nanoindentation tests of thin film on substrate, the thickness of the film beneath the indenter is smaller than its original value, because of plastic flow during loading. The use of the original film thickness t in the regression model cause a systematic shift or distortion of the Young's modulus curve. A correction proposed by Menčík et al. can be applied, assuming a rigid substrate and determining the effective thickness t_{eff} (in m)[34],[45],[10],[2] and[32].

$$\pi a^2 t_{\mathrm{eff}} = \pi a^2 t - V \tag{1.41}$$

With V the volume displaced by the indenter and approximated by $\pi a^2 h_{\mathrm{c}}/3$, for a conical indenter and contact depths h_{c} smaller than the film thickness.

$$t_{\mathrm{eff}} = t - \frac{h_{\mathrm{c}}}{3} \tag{1.42}$$

Recently, Li et al. proposed to express the local thinning effect as[32]:

[9] Chen X. and Vlassak J.J., "Numerical study on the measurement of thin film mechanical properties by means of nanoindentation." (2001).
[34] Menčík J. et al., "Determination of elastic modulus of thin layers using nanoindentation" (1997).
[45] Saha R. and Nix W.D., "Effects of the substrate on the determination of thin film mechanical properties by nanoindentation" (2002).
[10] Chen S. et al., "Nanoindentation of thin-film-substrate system: Determination of film hardness and Young's modulus" (2004).
[2] Bec S. et al., "Improvements in the indentation method with a surface force apparatus" (2006).
[32] Li H. et al., "New methods of analyzing indentation experiments on very thin films" (2010).

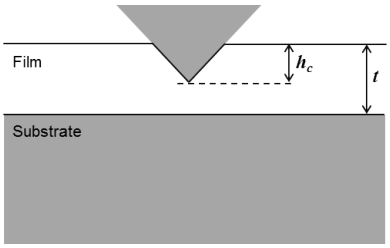

Figure 1.23: *Indentation penetration of a thin film on a sample.*

$$t_{\text{eff}} = t - \eta h_{\text{c}} \tag{1.43}$$

With η a parameter depending on the mechanical properties of the film and the substrate, and on the geometry of the indenter. Preliminary finite element calculations show that η should be independent of indentation depth and that its value ranges from 0.3 to 0.7 for materials that do not work harden.

1.4.2 Elastic properties of a thin film on a substrate

Several models to analyse indentation tests on bilayer sample and multilayer sample and to extract intrinsic material properties of the upper film (or the top coating) are detailed in the following part.

Some of the following models developed are detailed in the chapter 8 (“Nanoindentation of Thin Films”) of the book “Nanoindentation” written by A.C. Fischer-Cripps[15].

Bückle (1961)

Bückle proposed an empirical law (“rule of thumb”) to characterize thick coatings on a substrate[3]. It is possible to estimate the Young’s modulus of the coating for indentation depth lower than “10

Doerner and Nix (1986)

The model of Doerner and Nix is detailed in many papers[12],[29],[41] and[45], and is described by the following equation :

$$\frac{1}{E'} = \frac{1}{E'_{\text{f}}} + \left(\frac{1}{E'_{\text{s}}} - \frac{1}{E'_{\text{f}}} \right) e^{-\alpha(x)} \tag{1.44}$$

With $x = t/h_{\text{c}}$ and α an empirically constant determined using the method of least squares.

The equation was modified by King[29] with the replacement of t/h_{c} by t/a_{c}, and then by Saha and Nix[45] with the replacement of t/h_{c} by $(t - h_{\text{c}})/a_{\text{c}}$.

An empirical formulae based on the model of Doerner and Nix was proposed by Chen et al. in 2004[10]:

[15] Fischer-Cripps, A.C., “Nanoindentation 3rd Ed.” (2011)
[3] Bückle H., “VDI Berichte” (1961).
[12] Doerner M.F. and Nix W.D., “A method for interpreting the data from depth-sensing indentation instruments” (1986).
[29] King R.B., “Elastic analysis of some punch problems for a layered medium” (1987).
[41] Pharr G.M. and Oliver W.C., “Measurement of Thin Film Mechanical Properties Using Nanoindentation” (1992).

$$\frac{1}{E'} = \frac{1}{E_{\mathrm{f}}'}\left[1 - e^{-\alpha(x)^{(2/3)}}\right] + \frac{1}{E_{\mathrm{s}}'}e^{-\alpha(x)^{(2/3)}} \tag{1.45}$$

With $x = t/h_{\mathrm{c}}$ and α an empirically constant determined using the method of least squares.

Find here the Matlab function for the Doerner and Nix model[12]: model_doerner_nix.m.

Find here the Matlab function for the Doerner and Nix model modified by King[29]: model_doerner_nix_king.m.

Find here the Matlab function for the Doerner and Nix model modified by Saha[45]: model_doerner_nix_saha.m.

Find here the Matlab function function for the Doerner and Nix model modified by Chen[10]: model_chen.m.

Gao et al. (1992)

The model of Gao is described by the following equation[16] :

$$E^{'} = E_{\mathrm{s}}^{'} + \left(E_{\mathrm{f}}^{'} - E_{\mathrm{s}}^{'}\right)\phi_{Gao_0}(x) \tag{1.46}$$

$$\phi_{Gao_0} = \frac{2}{\pi}arctan\frac{1}{x} + \frac{1}{2\pi\left(1-\nu_{\mathrm{c}}\right)}\left[\left(1-2\nu_{\mathrm{c}}\right)\frac{1}{x}ln\left(1+x^2\right) - \frac{x}{1+x^2}\right] \tag{1.47}$$

$$\nu_c = 1 + \left[\frac{\left(1-\nu_{\mathrm{s}}\right)\left(1-\nu_{\mathrm{f}}\right)}{1-\left(1-\phi_{Gao_1}\right)\nu_{\mathrm{f}} - \phi_{Gao_1}\nu_{\mathrm{s}}}\right] \tag{1.48}$$

With ν_c the composite Poisson's ratio, ν_s the Poisson's ratio of the substrate and ν_f the Poisson's ratio of the thin film.

$$\phi_{Gao_1} = \frac{2}{\pi}arctan\frac{1}{x} + \frac{1}{x\pi}ln\left(1+x^2\right) \tag{1.49}$$

With $x = a_{\mathrm{c}}/t$.

Find here the Matlab function for the weighting function ϕ_{Gao_0} : phi_gao_0.m.

Find here the Matlab function for the weighting function ϕ_{Gao_1} : phi_gao_1.m.

Find here the Matlab function for ν_c the composite Poisson's ratio : composite_poissons_ratio.m.

Find here the Matlab function for the Gao et al. model : model_gao.m.

Menčík et al. (1997)

Menčík et al. proposed the following structures to express the combination of $E_{\mathrm{f}}^{'}$ and $E_{\mathrm{s}}^{'}$[34].

$$E^{'} = E_{\mathrm{s}}^{'} + \left(E_{\mathrm{f}}^{'} - E_{\mathrm{s}}^{'}\right)\phi(x) \tag{1.50}$$

$$E^{'} = E_{\mathrm{s}}^{'} + \left(E_{\mathrm{f}}^{'} - E_{\mathrm{s}}^{'}\right)\psi(x) \tag{1.51}$$

[16] Gao H. et al., "Elastic contact versus indentation modeling of multi-layered materials" (1992).

Where x is the ratio of the contact radius (a_c) or the contact depth (h_c), to the film thickness (t), and ϕ and ψ are weight functions of the relative penetration x. ϕ is equal to 1 when x is equal to 0 and 0 when x is infinite.

Note: If the difference between Poisson's ratio of the thin film and substrate is small, the values for uniaxial loading Young's moduli, E, E_f, E_s can be used in previous equation.

Menčík et al. (linear model) (1997)

Menčík described too the linear model by the following expression[34] :

$$E^{'} = E_f^{'} + \left(E_s^{'} - E_f^{'}\right)(x) \tag{1.52}$$

With $x = a_c/t$.

Find here the Matlab function for the Menčík et al. linear function : model_menick_linear.m.

Menčík et al. (exponential model) (1997)

Menčík described the exponential model by the following expression[34] :

$$E^{'} = E_s^{'} + \left(E_f^{'} - E_s^{'}\right) e^{-\alpha(x)} \tag{1.53}$$

With $x = a_c/t$ and α is an empirically constant determined using the method of least squares.

Find here the Matlab function for the Menčík et al. exponential function : model_menick_exponential.m.

Menčík et al. (reciprocal exponential model) (1997)

Menčík described the reciprocal exponential model by the following expression[34] :

$$\frac{1}{E'} = \frac{1}{E_s'} + \left(\frac{1}{E_f'} - \frac{1}{E_s'}\right) e^{-\alpha(x)} \tag{1.54}$$

With $x = a_c/t$ and α is an empirically constant determined using the method of least squares.

Find here the Matlab function for the Menčík et al. reciprocal exponential function : model_menick_reciprocal_exponential.m.

Perriot et al. (2003)

The following system of equation describes the model developed by Perriot et al.[40] :

[40] Perriot A. and Barthel E., "Elastic contact to a coated half-space: Effective elastic modulus and real penetration" (2004).

$$E^{'} = E_{\mathrm{f}}^{'} + \frac{E_{\mathrm{s}}^{'} - E_{\mathrm{f}}^{'}}{1 + \left(\frac{k_0}{x}\right)^n} \tag{1.55}$$

$$log(k_0) = -0.093 + 0.792log\left(\frac{E_{\mathrm{s}}^{'}}{E_{\mathrm{f}}^{'}}\right) + 0.05\left[log\frac{E_{\mathrm{s}}^{'}}{E_{\mathrm{f}}^{'}}\right]^2 \tag{1.56}$$

With $x = a_{\mathrm{c}}/t$, and k_0 and n are adjustable constants determined using the method of least squares.

Find here the Matlab function for the Perriot et al. model : model_perriot_barthel.m.

Jung et al. (2004)

Jung et al.[27] have adapted for conical indentation of thin films, the simple empirical approach of Hu and Lawn[21] developed initially for spherical indentation on bilayer structures. The following power-law relationship allows the evaluation of the Young's modulus of a thin film deposited on a substrate from nanoindentation experiments :

$$E = E_{\mathrm{s}}\left(\frac{E_{\mathrm{f}}}{E_{\mathrm{s}}}\right)^L \tag{1.57}$$

with L is the exponent term described by a dimensionless function :

$$L = \frac{1}{[1 + Ax^B]} \tag{1.58}$$

With $x = h_{\mathrm{c}}/t$ and where A and B are adjustable coefficients.

Jung et al. founded $A = 3.76$ and $B = 1.38$ after regression fits of (1.57) to different data sets. These coefficients are not universal and need to be "calibrated" with experimental data or with finite element data for specified material systems.

Finally, to be more consistent with other analytical models implemented in this toolbox, the model of Jung is modified by using the reduced form of the Young's moduli :

$$E^{'} = E_{\mathrm{s}}^{'}\left(\frac{E_{\mathrm{f}}^{'}}{E_{\mathrm{s}}^{'}}\right)^L \tag{1.59}$$

Find here the Matlab function for the sigmoidal function used in the Jung's model : sigmoidal_jung.m.

Find here the Matlab function for the Jung et al. model : model_jung.m.

Bec et al. (2006)

The elastic model of Bec et al. is based on indentation by a rigid cylindrical punch (radius a_{c}) of a homogeneous film deposited on a semi-infinite half space[2].

This system is modelled by two springs connected in series :

Find here the Matlab function for the Bec et al. model : model_bec.m.

[27] Jung Y.-G. et al. "Evaluation of elastic modulus and hardness of thin films by nanoindentation" (2004).
[21] Hu X.Z. and Lawn B. R. "A simple indentation stress–strain relation for contacts with spheres on bilayer structures" (1998).

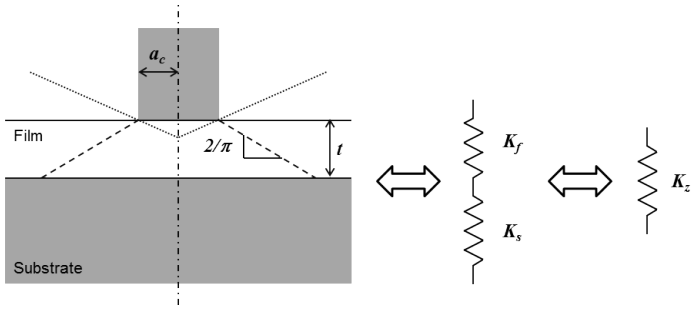

Figure 1.24: *Schematic description of the bilayer model of Bec et al.*

$$K_{\mathrm{f}} = \pi a_{\mathrm{c}}^2 \frac{E_{\mathrm{f}}^{'}}{t} \tag{1.60}$$

$$K_{\mathrm{s}} = 2a_{\mathrm{c}} E_{\mathrm{s}}^{'} \tag{1.61}$$

$$K_{\mathrm{z}} = 2a_{\mathrm{c}} E^{'} \tag{1.62}$$

$$\frac{1}{K_{\mathrm{z}}} = \frac{1}{f_{\mathrm{f}}\left(a_{\mathrm{c}}\right) K_{\mathrm{f}}} + \frac{1}{f_{\mathrm{s}}\left(a_{\mathrm{c}}\right) K_{\mathrm{s}}} \tag{1.63}$$

$$f_{\mathrm{f}}\left(a_{\mathrm{c}}\right) = f_{\mathrm{s}}\left(a_{\mathrm{c}}\right) = 1 + \frac{2t}{\pi a_{\mathrm{c}}} \tag{1.64}$$

$$\frac{1}{2a_{\mathrm{c}}E'} = \frac{t}{\left(\pi a_{\mathrm{c}}^2 + 2ta_{\mathrm{c}}\right) E_{\mathrm{f}}^{'}} + \frac{1}{2\left(a_{\mathrm{c}} + \frac{2t}{\pi}\right) E_{\mathrm{s}}^{'}} \tag{1.65}$$

Korsunsky and Constantinescu (2009)

Korsunsky and Constantinescu proposed a simple model response function to the analysis of indentation of elastic coated systems[30] and[31]. They expressed the reduced Young's modulus in terms of a linear law of mixtures of the form:

$$E^{'} = E_1^{'} + \frac{E_2^{'} - E_1^{'}}{1 + \left(\frac{h_{\mathrm{t}}}{\beta_0 t}\right)^{\eta}} \tag{1.66}$$

Here $E_1^{'}$, $E_2^{'}$, η and β_0 are positive constants to be determined from fitting. It may be expected that for very shallow indentation ($\beta_0 \ll 1$), the corresponding parameter $E_1^{'}$ ought to approach the Young's modulus of the coating $E_{\mathrm{f}}^{'}$. Similarly, one might also expect that for very deep indentation ($\beta_0 \gg 1$), the corresponding parameter $E_2^{'}$ ought to approach the Young's modulus of the substrate $E_{\mathrm{s}}^{'}$. Values of η and β_0 depend on the indentation boundary condition, if the coating is a defined as a freely sliding layer or as a perfectly bonded layer.

Hay et al. (2011)

The present model of Hay et al.[19] is a development of the Song–Pharr model[44] and[48], which is already inspired by the Gao model[16].

[30] Korsunsky A.M. et al. "On the hardness of coated system" (1998).
[31] Korsunsky A.M. and Constantinescu A., "The influence of indenter bluntness on the apparent contact stiffness of thin coatings" (2009).
[19] Hay J. and Crawford B., "Measuring substrate-independent modulus of thin films" (2011).
[44] Rar A. et al., "Assessment of new relation for the elastic compliance of a film–substrate system." (2002).
[48] Xu H. and Pharr G.M., "An improved relation for the effective elastic compliance of a film/substrate system during indentation by a flat cylindrical punch." (2006).

$$\frac{1}{\mu_c} = (1 - \phi_{Gao_0}) \frac{1}{\mu_s + F\phi_{Gao_0}\mu_f} + \phi_{Gao_0} \frac{1}{\mu_f} \tag{1.67}$$

Where μ_c (in GPa $=$ N/m^2) is the composite shear modulus calculated from the composite Young's modulus as :

$$\mu_c = \frac{E}{2(1 + \nu_c)} \tag{1.68}$$

Where ν_c is the composite Poisson's ratio given in Gao's model.

$$E = \left(1 - \nu_c^2\right) E^{'} \tag{1.69}$$

Knowing μ_c, it is possible to calculate μ_f :

$$\mu_f = \frac{-B + \sqrt{B^2 - 4AC}}{2A} \tag{1.70}$$

Where $A = F\phi_{Gao_0}$

$$B = \mu_s - \left(F\phi_{Gao_0}^2 - \phi_{Gao_0} + 1\right) \mu_c \tag{1.71}$$

With $F = 0.0626$, a constant obtained from finite element simulations.

$$C = -\phi_{Gao_0}\mu_c\mu_s \tag{1.72}$$

$$\mu_s = \frac{E_s}{2(1 + \nu_s)} \tag{1.73}$$

Finally, the Young's modulus of the film is calculated from the shear modulus and Poisson's ratio of the film :

$$E_f = 2\mu_f (1 + \nu_f) \tag{1.74}$$

Find here the Matlab function for the Hay et al. model : model_hay.m.

Bull (2014)

This model was originally proposed by Bull S.J. in 2011, in a paper about the mechanical characterization of ALD Alumina coatings[5]. Then, this simple method to determine the elastic modulus of a coating on a substrate using nanoindentation was developed in another paper in 2014[6]. This model is based on the load support of a truncated cone of material beneath the indenter.

[5] Bull S.J., "Mechanical response of atomic layer deposition alumina coatings on stiff and compliant substrates" (2011).
[6] Bull S.J., "A simple method for the assessment of the contact modulus for coated systems." (2014).

$$E^{'} = \frac{F_{\mathrm{c}}}{2a_{\mathrm{c}}\left(h_{\mathrm{c}} + h_{\mathrm{s}}\right)} \tag{1.75}$$

$$h_{\mathrm{c}} = \frac{F_{\mathrm{c}}}{\pi E_{\mathrm{f}}}\left[\frac{1}{a_{\mathrm{c}} tan\alpha} - \frac{1}{a_{\mathrm{c}} tan\alpha + t_{\mathrm{f}} tan^2\alpha}\right] \tag{1.76}$$

$$h_{\mathrm{s}} = \frac{F_{\mathrm{c}}}{\pi E_{\mathrm{s}}}\left[\frac{1}{a_{\mathrm{c}} tan\alpha + t_{\mathrm{f}} tan^2\alpha} - \frac{1}{a_{\mathrm{c}} tan\alpha + (t_{\mathrm{f}} + t_{\mathrm{s}}) tan^2\alpha}\right] \tag{1.77}$$

Where E_{f} and E_{s} are the Young's Modulus of the coating and substrate, t_{f} and t_{s} are the coating and substrate thickness, and α is the semi-angle of the cone material which supports the load. In fact, by assuming that the material thickness is very much greater than the contact radius, it is possible to replace in the previous equation $tan\alpha$ by $2\pi = 32.48$. Finally, by assuming that the substrate is very much thicker than the coating ($t_{\mathrm{s}} >> t_{\mathrm{f}}$), the equation (1.75) can be rewritten :

$$E^{'} = \frac{1}{\frac{1}{E_{\mathrm{f}}}\left[\frac{2t_{\mathrm{f}}}{\pi a_{\mathrm{c}} + 2t_{\mathrm{f}}}\right] + \frac{1}{E_{\mathrm{s}}}\left[\frac{\pi a_{\mathrm{c}}}{\pi a_{\mathrm{c}} + 2t_{\mathrm{f}}}\right]} \tag{1.78}$$

This last equation from Bull S.J. is exactly the same as equation (1.65), proposed by Bec et al. in 2006, with a unique difference which is the use by Bull S.J. of the non reduced form of the Young's moduli of the coating and the substrate.

1.4.3 Elastic properties of a thin film on a multilayer system

In 2008, Pailler-Mattei et al. proposed an extension of the Bec's model to a bilayer system deposited on a substrate[39].

But more recently, Mercier et al. established a generalization of the Bec's model to $N + 1$ layers sample.

Mercier et al. (2010)

The elastic model of Mercier et al. for a multilayer sample on $N + 1$ layers is an extension of the Bec et al. model[35] and[36].

$$\frac{1}{2a_{\mathrm{c},0}E'} = \sum_{i=0}^{N} \frac{t_i}{\left(\pi a_{\mathrm{c},i}^2 + 2t_i a_{\mathrm{c},i}\right) E'_{\mathrm{f},i}} + \frac{1}{2\left(a_{\mathrm{c},N} + \frac{2t_N}{\pi}\right) E'_{\mathrm{s}}} \tag{1.79}$$

$$a_{\mathrm{c},i+1} = a_{\mathrm{c},i} + \frac{2t}{\pi} \tag{1.80}$$

With $a_{\mathrm{c},0}$ equal to a_{c}.

Thus, the Young's modulus of the film can be calculated as :

$$E'_{\mathrm{f},0} = \left[\frac{\pi a_{\mathrm{c},0}^2 + 2t_0 a_{\mathrm{c},0}}{t_0}\left[\frac{1}{2a_{\mathrm{c},0}E'} - \left(\sum_{i=1}^{N} \frac{t_i}{\left(\pi a_{\mathrm{c},i}^2 + 2t_i a_{\mathrm{c},i}\right) E'_{\mathrm{f},i}} + \frac{1}{2\left(a_{\mathrm{c},N} + \frac{2t_N}{\pi}\right) E'_{\mathrm{s}}}\right)\right]\right]^{-1} \tag{1.81}$$

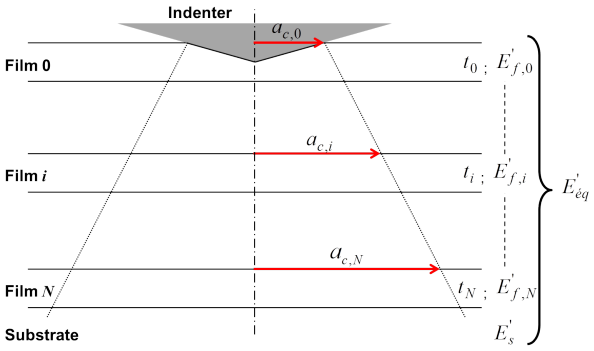

Figure 1.25: *Schematic of elastic multilayer model.*

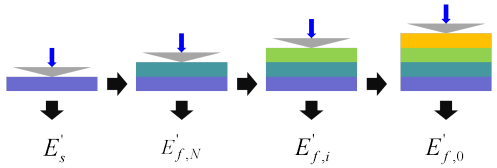

Figure 1.26: *Experimental process to apply for elastic multilayer model.*

It is advised to perform nanoindentation tests on each layer of the multilayer sample, from the substrate up to the final stack of layers (see Figure 1.26). By successive iterations using the model of Mercier et al., values of Young's modulus of each layer are extracted from the contact stiffness.

Find here the Matlab function for the Mercier et al. model : model_multilayer_elastic.m.

Puchi-Cabrera et al. (2015)

Puchi-Cabrera et al. proposed in 2015, a description of the composite elastic modulus of multilayer coated systems[42], based on the physically-based concept advanced by Rahmoun et al.[43] :

$$\frac{1}{E} = \sum_{i=1}^{N} \frac{x_{\mathrm{v}}^{\mathrm{i}}}{E_{\mathrm{f}}^{\mathrm{i}}} + \frac{x_{\mathrm{v}}^{\mathrm{s}}}{E_{\mathrm{s}}} \tag{1.82}$$

With $x_{\mathrm{v}}^{\mathrm{i}}$ and $x_{\mathrm{v}}^{\mathrm{s}}$, respectively the volume fraction of each layer and the corresponding volume fraction of the substrate material. In his paper, Puchi-Cabrera modified and extended from the bilayer to the multilayer specimen, the models of Doerner and Nix, Gao, Bec, Menčík, Perriot and Barthel, Antunes, Korsunsky and Constantinescu and Bull.

1.4.4 Plastic properties of a thin film on a substrate

It is possible to estimate empirically the hardness of the coating for indentation depth lower than "40

[39] Pailler-Mattei C. et al., "In vivo measurements of the elastic mechanical properties of human skin by indentation tests" (2008).
[35] Mercier D. et al., "Young's modulus measurement of a thin film from experimental nanoindentation performed on multilayer systems" (2010).
[36] Mercier D., "Behaviour laws of materials used in electrical contacts for « flip chip » technologies" (2013).
[42] Puchi-Cabrera. E.S. et al., "A description of the composite elastic modulus of multilayer coated systems" (2015).
[43] Rahmoun K. et al., "A multilayer model for describing hardness variations of aged porous silicon low-dielectric-constant thin films" (2009).

Bückle (1961)

Bückle proposed an expression of the composite hardness H in the case of a two-layer material with a weighted sum of the different layer hardnesses during indentation process[3].

$$H = aH_{\mathrm{f}} + bH_{\mathrm{s}} \tag{1.83}$$

With H_{f} the hardness of the film, H_{s} the hardness of the substrate and $a + b = 1$. a varies from 1 when the hardness is not affected by the substrate, to 0 when the indentation depth is approaching the film thickness.

Kao and Byrne (1981)

Kao and Byrne proposed the following model to describe the evolution of the composite hardness in function of the reciprocal indentation depth[28], based on Bückle's model[3] :

$$H \simeq H_{\mathrm{s}} + 2k_1 t_{\mathrm{f}} \left(H_{\mathrm{f}} - H_{\mathrm{s}}\right) \frac{1}{h} \tag{1.84}$$

With k_1 a weighting factor of about 9%, independent of material characteristics.

Jönsson and Hogmark (1984)

Jönsson and Hogmark used a simple geometrical approach based on a area "law of mixtures" to separate the substrate and film contributions to the measured hardness from Vickers indentation[25].

$$H = \frac{A_{\mathrm{f}}}{A} H_{\mathrm{f}} + \frac{A_{\mathrm{s}}}{A} H_{\mathrm{s}} \tag{1.85}$$

With A_{f} the area on which the mean pressure H_{f} acts and A_{s} the area on which the mean pressure H_{s} acts. The total area A is the sum of A_{f} and A_{s} and the following expressions for the area ratios are given by Jönsson and Hogmark:

$$\frac{A_{\mathrm{f}}}{A} = 2C\frac{t}{d} - C^2\frac{t}{d}^2 \tag{1.86}$$

$$\frac{A_{\mathrm{s}}}{A} = 1 - \frac{A_{\mathrm{f}}}{A} \tag{1.87}$$

With d the diagonal of the indent, t the film thickness and C a constant equal to 0.5 for hard coatings on very soft substrates ($6.3 < \frac{H_{\mathrm{f}}}{H_{\mathrm{s}}} < 12.9$) or to 1 when the coatings and substrate hardnesses are more similar ($1.8 < \frac{H_{\mathrm{f}}}{H_{\mathrm{s}}} < 2.3$).

[22]

[28] Kao P.-W. and Byrne J. G., "Ion Implantation Effects on Fatigue and Surface Hardness" (1981).
[25] Jönsson B. and Hogmark S., "Hardness measurements of thin films" (1984).
[22] Iost A. and Bigot R., "Hardness of coatings" (1996).

Burnett and Rickerby (1984)

Burnett and Rickerby proposed afterwards a model based on a "volume law of mixtures" similar to Jönsson's relation, considering the volumes of the plastic zones, V_f and V_s respectively in the film and in the substrate[78].

$$H = \frac{V_\mathrm{f}}{V} H_\mathrm{f} + \frac{V_\mathrm{s}}{V} H_\mathrm{s} \tag{1.88}$$

With $V = V_\mathrm{f} + V_\mathrm{s}$.

Chicot and Lesage (1995)

"volume law of mixtures"

11

20

30

14

Saha and Nix (2002)

Based on the methodology proposed by Joslin and Oliver (1990)[26] for a bulk material, extended to the coated system by Page et al.[38], Saha and Nix proposed to use the following equation, giving the evolution of the hardness in function of indentation depth, even when pile-up occurs[45]:

$$H = \beta^2 \frac{4}{\pi} \frac{F_{\mathrm{c,max}}}{S^2} (E*)^2 \tag{1.89}$$

$$\frac{1}{E^*} = \frac{1}{E_\mathrm{i}'} + \frac{1}{E_\mathrm{f}'} + \left(\frac{1}{E_\mathrm{s}'} - \frac{1}{E_\mathrm{f}'} \right) e^{-\alpha(x)} \tag{1.90}$$

With $x = (t - h_\mathrm{c})/a_\mathrm{c}$ and E_i' the reduced Young's modulus of the indenter.

This model was reused later by Han et al.[17] and[18].

Note: This model is valid only for the case of elastically inhomogeneous film/substrate systems.

Chen (2004)

10

[7] Burnett P.J. and Rickerby D.S., "The mechanical properties of wear-resistant coatings: I: Modelling of hardness behaviour." (1987).
[8] Burnett P.J. and Rickerby D.S., "The mechanical properties of wear-resistant coatings: II: Experimental studies and interpretation of hardness." (1987).
[11] Chicot D. and Lesage J., "Absolute hardness of films and coatings" (1995).
[20] He J.L. et al., "Hardness measurement of thin films: Separation from composite hardness" (1996).
[14] Fernandes J.V. et al., "A model for coated surface hardness" (2000).
[26] Joslin D.L. and Oliver W.C., "A new method for analyzing data from continuous depth-sensing microindentation tests" (1990).
[38] Page T.F. et al., "Nanoindentation Characterisation of Coated Systems: P:S2 - A New Approach Using the Continuous Stiffness Technique" (1998).
[17] Han S.M. et al., "Combinatorial studies of mechanical properties of Ti–Al thin films using nanoindentation" (2005).
[18] Han S.M. et al., "Determining hardness of thin films in elastically mismatched film-on-substrate systems using nanoindentation" (2006).

Iost (2005)

[23]

1.4.5 Plastic properties of a thin film on a multilayer system

Engel et al. (1992)

Engel et al. proposed a simple method of interpreting the superficial (Vickers) hardness of multilayered specimen[13], by expanding the concept of Jönsson and Hogmark[25] :

$$H = \frac{A_\mathrm{s}}{A} H_\mathrm{s} + \sum_{i=1}^{N} \frac{A_\mathrm{f,i}}{A} H_\mathrm{f,i} \tag{1.91}$$

$$A = A_\mathrm{s} + \sum_{i=1}^{N} A_\mathrm{f,i} \tag{1.92}$$

With N the number of layers deposited on the substrate, $A_\mathrm{f,i}$ and $H_\mathrm{f,i}$ respectively the flow pressure area and the hardness of an intermediate layer. According to the author, this model is applicable as long as the ratio of the film thickness t_f over the indentation imprint size (i.e. the diagonal d of square imprint in case of Vickers indentation) is less than 0.2, resulting in a parallel displacement of indenter, layers, and substrate.

Rahmoun et al. (2009)

[43]

$$H = \frac{A_\mathrm{f}}{A} H_\mathrm{f} + \frac{A_\mathrm{i}}{A} H_\mathrm{i} + \frac{A_\mathrm{s}}{A} H_\mathrm{s} \tag{1.93}$$

$$\frac{A_\mathrm{f}}{A} = \frac{2t_\mathrm{f}}{h} - \frac{t_\mathrm{f}^2}{h^2} \tag{1.94}$$

$$\frac{A_\mathrm{i}}{A} = \frac{2t_\mathrm{f}}{h} - \frac{t_\mathrm{i}^2}{h^2} - 2\frac{t_\mathrm{i} t_\mathrm{f}}{h^2} \tag{1.95}$$

$$\frac{A_\mathrm{s}}{A} = 1 - \frac{2(t_\mathrm{f} + t_\mathrm{i})}{h} + \frac{(t_\mathrm{f} + t_\mathrm{i})^2}{h^2} \tag{1.96}$$

Arrazat et al. (2010)

[1]

[23] Iost A. et al., “Dureté des revêtements : quel modèle choisir ?” (2005).
[13] Engel P.A. et al., “Interpretation of superficial hardness for multilayer platings*” (1992).
[1] Arrazat B. et al., “Nano indentation de couches dures ultra minces de ruthénium sur or” (2010).

1.4.6 References

1.5 Examples of nanoindentation data

Please look at the experimental procedure proposed by Jennett N. M. and Bushby A. J.[1], to perform nanoindentation tests on bulk, coatings or multilayer systems, and to the ISO standard (ISO 14577 - 1 to 4).

1.5.1 Type of data - Pre-Requirements

Only data continuously measured in function of the indentaton depth are accepted in the NIMS toolbox (e.g.: CSM mode for Agilent - MTS nanoindenter or DMA - CMX algorithm for Hysitron nanoindenter).

You data must only have the loading part from the load-displacement curves of your (nano)indentation results. In the case of data saved in a 'Sample' or 'Analyst Project' sheet of a .xls file obtained with 'Analyst' (MTS software) (containing at least a 'Hold Segment Type' or a 'END' segment), the toolbox is able to consider only the loading part of your results.

Please, check if the surface detection is well done, especially if the substrate is compliant[2] and[4]. For more explanations about the surface detection, look into the NIMS documentation.

It is advised to use average results from at least 10 indentation tests to avoid artefacts (e.g. pop-in, roughness, local impurities or dust on the sample's surface...).

Note: To analyze pop-in distribution, the Matlab PopIn toolbox was developed. The Matlab code is available on GitHub with the documentation.

1.5.2 Agilent - MTS example files

- Both .txt or .xls files are accepted.
- 3 columns (Displacement / Load / Stiffness)
- 6 columns (Disp. / SD (Disp.) / Load / SD (Load.) / Stiff. / SD (Stiff.)) (SD for Standard Deviation)
- **MTS_0film_Si_CSM-2nm_noSD.txt**
  - Data for a bulk Silicon sample.
  - Data obtained by Berkovich indentation with CSM mode (75Hz / amplitude 2nm) (no standard deviation).
- **MTS_1film_SiO2_Si_CSM-2nm.xls**
  - Data for a thin film of Silicon thermal oxide (500nm) on a bulk Silicon sample.
  - Data obtained by Berkovich indentation with CSM mode (75Hz / amplitude 2nm).
- **MTS_1film_SiO2_Si_CSM-2nm_noSD.xls**
  - Data for a thin film of Silicon thermal oxide (500nm) on a bulk Silicon sample.
  - Data obtained by Berkovich indentation with CSM mode (75Hz / amplitude 2nm) (no standard deviation).

[1] Jennett N. M. and Bushby A. J., "Adaptive Protocol for Robust Estimates of Coatings Properties by Nanoindentation" (2001).
[2] Kaufman J. D. and Klapperich C. M., "Surface detection errors cause overestimation of the modulus in nanoindentation on soft materials" (2009).
[4] Piccarolo S. et al., "Improving surface detection on nanoindentation of compliant materials" (2010).

- **MTS_2films_Al_SiO2_Si_CSM-2nm.xls**
  - Data for a thin film of PVD Aluminum (500nm) deposited on a bulk Silicon sample with a Silicon thermal oxide (500nm).
  - Data obtained by Berkovich indentation with CSM mode (75Hz / amplitude 2nm).
- **MTS_3films_Au-Ti-SiO2-Si_CSM-1nm.txt**
  - Data for a thin film of PVD Gold (500nm) deposited on thin film of PVD Titanium (500nm) on a bulk Silicon sample with a Silicon thermal oxide (500nm).
  - Data obtained by Berkovich indentation with CSM mode (75Hz / amplitude 1nm).
- **MTS_3films_Au-Ti-SiO2-Si_CSM-1nm.xls**
  - Data for a thin film of PVD Gold (500nm) deposited on thin film of PVD Titanium (500nm) on a bulk Silicon sample with a Silicon thermal oxide (500nm).
  - Data obtained by Berkovich indentation with CSM mode (75Hz / amplitude 1nm).

The last example (2 files for Au-Ti-SiO2-Si sample) is used to validate the elastic multilayer model of Mercier et al.[3]. A micrograph of this sample is given Figure 1.27.

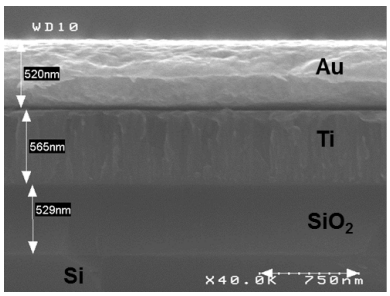

Figure 1.27: *SEM cross-sectional observation of a multilayer sample.*

1.5.3 Hysitron example files

- Both .txt or .dat files are accepted.
- **Hysitron_dma.txt**
  - Data obtained by Berkovich indentation with DMA mode (205Hz / amplitude 0.65nm (Courtesy of Dr. Igor Zlotnikov from Max Planck Institute of Colloids and Interfaces in Potsdam, Germany).

1.5.4 References

- ISO 14577 - 1 , "Metallic materials – Instrumented indentation test for hardness and materials parameters – Part 1: Test method", (2002).
- ISO 14577 - 2 , "Metallic materials – Instrumented indentation test for hardness and materials parameters – Part 2: Verification and calibration of testing machines", (2002).
- ISO 14577 - 3 , "Metallic materials – Instrumented indentation test for hardness and materials parameters – Part 3: Calibration of reference blocks", (2002).

[3] Mercier D. et al., "Young's modulus measurement of a thin film from experimental nanoindentation performed on multilayer systems" (2010).

- ISO 14577 - 4 , "Metallic materials – Instrumented indentation test for hardness and materials parameters – Part 4: Test method for metallic and non-metallic coatings", (2007).
- Agilent website
- Hysitron website

1.6 FEM model

1.6.1 Finite Element Modelling (FEM) of conical indentation

The present model is a simulation of the conical nanoindentation process, using the FEM software ABAQUS.

The Matlab function used to generate a Python script for ABAQUS is : python_abaqus

The model is axisymmetric with a geometry dependent mesh and restricted boundaries conditions.

Geometry of the (multilayer) sample

Each layer of the sample is characterized by its thickness (t_{i}).

The thickness of the substrate (t_{sub}) is set as 2 times the highest thin film thickness.

The width (w) of the sample is calculated in function of the substrate thickness or the indenter tip defect.

No delamination is allowed between thin films or between thin film and substrate.

Note: Dimensions are in nm.

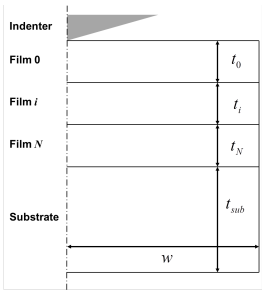

Figure 1.28: *Geometry of the sample in the FEM model.*

Geometry of the indenter

The indenter is defined as a rigid cono-spherical indenter. A spherical part is defined at the apex of the conical indenter (see Figure 1.29).

The radius R of the spherical part is calculated from the tip defect h_{tip} and the cone angle α, using the following equation. For Berkovich, Vickers and Cube-Corner indenters, the equivalent cone angle is used to set the cone angle.

$$R = \frac{h_{\mathrm{tip}}}{\frac{1}{sin(\alpha)} - 1} \tag{1.97}$$

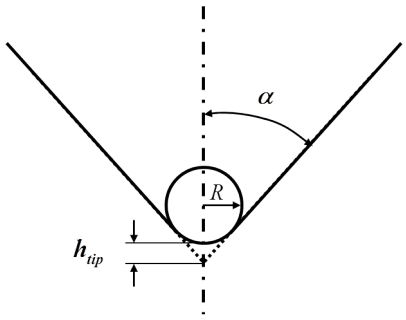

Figure 1.29: *Scheme of a cono-spherical indenter.*

In case, a perfect conical indenter is set in the GUI ($h_{\text{tip}} = 0$nm), the radius is calculated using a tip defect of 0.1nm by default, which gives a radius of $R = 1.6$nm.

Defining a spherical tip avoids the geometrical singularity at the apex of the perfect conical indenter, which would imply an infinite stress at the contact interface.

Mesh

The multilayer sample is divided by default into solid elements with eight nodes and axisymmetric deformation element CAX8R is adopted.

It is possible to divide the sample into solid elements with four nodes and with axisymmetric deformation element CAX4R, by changing the value of the variable "linear_elements" in the Matlab function python4abaqus from 0 (quadratic elements) to 1 (linear elements).

Note:

- CAX4R: A 4-node bilinear axisymmetric quadrilateral, reduced integration, hourglass control.
- CAX3: A 3-node linear axisymmetric triangle.
- CAX8R: An 8-node biquadratic axisymmetric quadrilateral, reduced integration.
- CAX6M: A 6-node modified quadratic axisymmetric triangle.

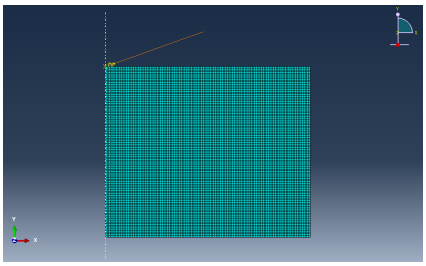

Figure 1.30: *Screenshot in Abaqus of the mesh example used in the FE model.*

Material properties

For each layers of the multilayer sample, the material properties (Young's modulus and Poisson's ratio) are defined using the inputs given by the user from the GUI. Material properties are considered by default to be isotropic. The density is set by default to 1.0.

Note: Young's moduli are in GPa.

Contact definition

The contact is defined by default frictionless for the tangential behavior and hard for the normal behavior.

The external surface of the indenter is defined as the "master" region and the top surface of the (multilayer) sample is defined as the "slave" region.

Note: Usually, the effect of friction may be neglected when indenter tips with half-angle larger than 60∘ are used (e.g.: Berkovich, Vickers)[1],[4],[2],[3].

Boundaries conditions

Nodes are constrained along the rotation axis from moving in the radial direction (x). The nodes on the bottom surface of the sample are constrained along the radial axis from moving in the radial (x) and vertical (z) directions (see Figure 1.31 and Figure 1.32).

Indentation process is simulated by imposing a vertical displacement to the rigid indenter along the (z) axis (see Figure 1.31 and Figure 1.32). A value of 200nm for the indentation depth is set by default.

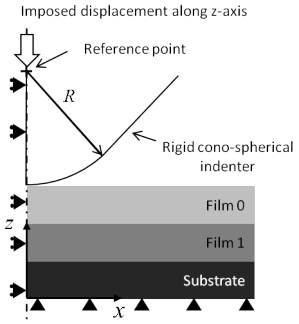

Figure 1.31: *Schematic of boundaries conditions used in the FE model.*

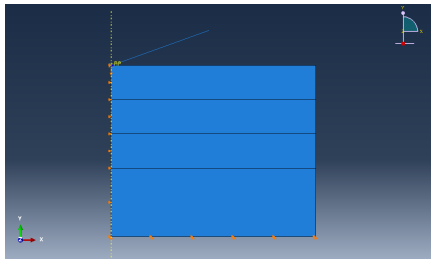

Figure 1.32: *Screenshot of the FE model with BCs in Abaqus.*

[1] Atkins A.G. and Tabor D., "Plastic indentation in metals with cones" (1965).
[4] Johnson K.L., "Contact Mechanics" (1987), ISBN - 9780521347969.
[2] DiCarlo A. et al., "Prediction of stress–strain relation using cone indentation: effect of friction" (2004).
[3] Harsono E. et al., "The effect of friction on indentation test results" (2008).

Warning: Indentation displacement is given in nanometers and is negative.

1.6.2 Generation of the Python script for ABAQUS

After material properties are configured (Young's moduli and Poisson's ratios) and the model geometry is given (thickness for each thin films), a Python script for ABAQUS can be generated by pressing the 'FEM' button.

The python script is saved in the folder where your nanoindentation results are stored.

To generate the FEM model in ABAQUS, apply the following procedure:

- start ABAQUS
- select the folder containing input files : 'File' ==> 'Set Work Directory...'
- select and run the Python file containing the FEM model (*.py) : File' ==> 'Run Script'

Note: Dimensions are in nm and Young's moduli are in GPa, implying that load is in nN.

1.6.3 Results of the FEM simulation

The following pictures were obtained for a multilayer Au/Ti/SiO2/Si.

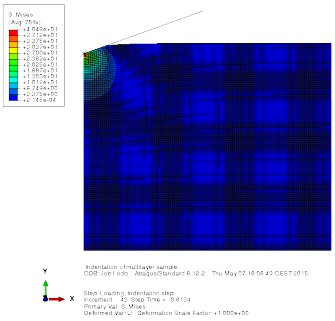

Figure 1.33: *Screenshot of the Von Mises stress distribution at maximum load.*

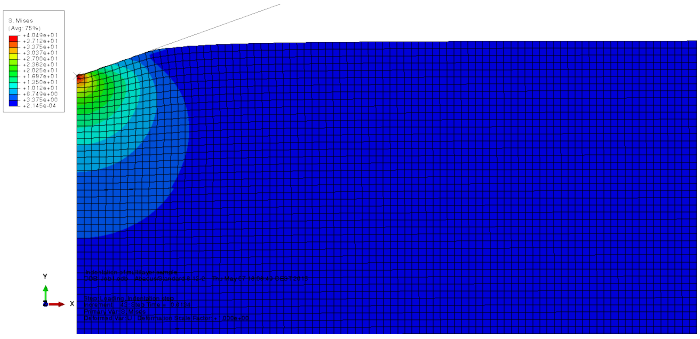

Figure 1.34: *Screenshot (with a zoom in on the contact area) of the Von Mises stress distribution at maximum load.*

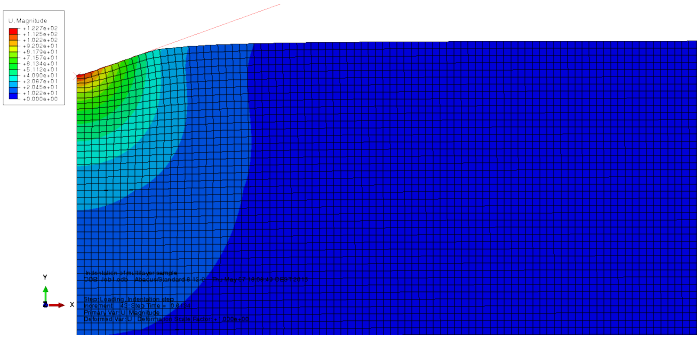

Figure 1.35: *Screenshot (with a zoom in on the contact area) of the magnitude of the displacement at maximum load.*

1.6.4 References

- ABAQUS documentation
- Charleux L., "Abapy Documentation"
- Bhattacharya A.K. and Nix W.D., "Finite element analysis of cone indentation." (1991).
- Madsen D.T. et al. "Finite Element Simulation of Indentation Behavior of thin Films." (1991).
- Sun Y. et al., "Finite element analysis of the critical ratio of coating thickness to indentation depth for coating property measurements by nanoindentation." (1995).
- Hubert N. et al. "Identification of elastic-plastic material parameters from pyramidal indentation of thin films." (2002).
- He J.L. and Veprek S., "Finite element modeling of indentation into superhard coatings." (2003).
- Cai X. and Bangert H., "Hardness measurements of thin films-determining the critical ratio of depth to thickness using FEM." (2005).
- Bolshakov A. and Pharr G.M., "Influences of pile-up on the measurement of mechanical properties by load and depth sensing indentation techniques." (1998)
- Lichinchi M. et al., "Simulation of Berkovich nanoindentation experiments on thin films using finite element method." (1998).
- Chen X. and Vlassak J.J., "A Finite Element Study on the Nanoindentation of Thin Films." (2000).
- Chen X. and Vlassak J.J., "Numerical study on the measurement of thin film mechanical properties by means of nanoindentation." (2001).
- Bouzakis K.-D. et al., "Thin hard coatings stress–strain curve determination through a FEM supported evaluation of nanoindentation test results.", (2001).
- Xu Z.-H. and Rowcliffe D., "Finite element analysis of substrate effects on indentation behaviour of thin films." (2004).
- Panich N. and Sun Y. "Effect of penetration depth on indentation response of soft coatings on hard substrates: a finite element analysis" (2004)
- Bressan J.D. et al., "Modeling of nanoindentation of bulk and thin film by finite element method." (2005).
- Pelletier H. et al., "Characterization of mechanical properties of thin films using nanoindentation test." (2006)
- Xu H., "A Finite Element Study of the Contact Stiffness of Homogenous Materials and Thin Films." PhD thesis - University of Tennessee - Knoxville (2007)
- Antunes J.M. et al., "On the determination of the Young's modulus of thin films using indentation tests" (2007).

- Chen S.H. et al., “Small scale, grain size and substrate effects in nano-indentation experiment of film–substrate systems.” (2007).
- Huang X. and Pelegri A.A., “Finite element analysis on nanoindentation with friction contact at the film/substrate interface.” (2007).
- Pelegri A.A. and Huang X., “Nanoindentation on soft film/hard substrate and hard film/soft substrate material systems with finite element analysis.” (2008).
- Wittler O. et al., “Mechanical characterisation of thin metal layers by modelling of the nanoindentation experiment.” (2008).
- Sakharova N.A. et al., “Comparison between Berkovich, Vickers and conical indentation tests: A three-dimensional numerical simulation study.” (2009).
- Chen C., “2-D Finite Element Modeling for Nanoindentation and Fracture Stress Analysis.” PhD thesis - University of South Florida (2009).
- Moore S.W. et al., “Nanoindentation in elastoplastic materials: insights from numerical simulations.” (2010).
- Dowhan L. et al., “Investigation of thin films by nanoindentation with doe and numerical methods.” (2011).
- Isselé H. et al., “Determination of the Young’s modulus of a TiN Thin Film by nanoindentation: analytical models and numerical FEM simulation.” (2012).
- Phiciato’s blog (2013)
- Moćko W. et al., “Simulation of nanoindentation experiments of single-layer and double-layer thin films using finite element method.” (2014).
- Kibech S. et al., “Nanoindentation” (2014).
- Kopernik M. and Milenin A., “Numerical modeling of substrate effect on determination of elastic and plastic properties of TiN nanocoating in nanoindentation test.” (2014).
- Li Y. et al., “Models for nanoindentation of compliant films on stiff substrates” (2015).
- Gupta A. K. et al., “Evaluation of elasto-plastic properties of ITO film using combined nanoindentation and finite element approach” (2015).

1.7 Links and References

1.7.1 Links

- Guidata on Matlab website.
- Matlab GUI.
- Coding GUI behavior.
- Visit the YAML website for more informations.
- Visit the YAML code for Matlab.

1.7.2 Links about (nano)indentation

- SF2M - Groupe Indentation.
- Matlab Li’s code to determine elastic modulus and hardness of an ultra-thin film on a substrate using nanoindentation.

- ISO 14577 - 1 , “Metallic materials – Instrumented indentation test for hardness and materials parameters – Part 1: Test method”, (2002).
- ISO 14577 - 2 , “Metallic materials – Instrumented indentation test for hardness and materials parameters – Part 2: Verification and calibration of testing machines”, (2002).
- ISO 14577 - 3 , “Metallic materials – Instrumented indentation test for hardness and materials parameters – Part 3: Calibration of reference blocks”, (2002).
- ISO 14577 - 4 , “Metallic materials – Instrumented indentation test for hardness and materials parameters – Part 4: Test method for metallic and non-metallic coatings”, (2007).

1.7.3 References

- Mercier D. et al., “Young’s modulus measurement of a thin film from experimental nanoindentation performed on multilayer systems” (2010).
- Mercier D., “Behaviour laws of materials used in electrical contacts for « flip chip » technologies.”, PhD thesis (2013)
- Mercier D., “Behaviour laws of materials used in electrical contacts for « flip chip » technologies.” PhD defense (2013).

(Nano)Indentation models (conical indenters)

- Love A.E.H., “Boussinesq’s problem for a rigid cone.” (1939).
- Galin L.A., “Spatial contact problems of the theory of elasticity for punches of circular shape in planar projection.”, J. Appl. Math. Mech. (PMM) (1946), 10, pp. 425-448.
- Bulychev S.I. et al., “Determining Young’s modulus from the indentor penetration diagram.”, Zavod. Lab., 1973, 39, pp. 1137-1142.
- Shorshorov M.K. et al., Sov. Phys. Dokl., 1982, 26.
- Loubet J.L. et al., “Vickers Indentation Curves of Magnesium Oxide (MgO).” (1984).
- Doerner M.F. and Nix W.D., “A method for interpreting the data from depth-sensing indentation instruments” (1986).
- Loubet J.L. et al., “Vickers indentation curves of elastoplastic materials” (1986).
- Joslin D.L. and Oliver W.C., “A new method for analyzing data from continuous depth-sensing microindentation tests” (1990).
- Oliver W.C. and Pharr G.M., “An improved technique for determining hardness and elastic modulus using load and displacement sensing indentation experiments” (1992).
- Pharr G.M. et al., “On the generality of the relationship among contact stiffness, contact area, and elastic modulus during indentation” (1992).
- Loubet J.L. et al., “Nanoindentation with a surface force apparatus.” (1993).
- Lucas B.N. et al., “Time Dependent Deformation During Indentation Testing.” (1996).
- Hainsworth S.V. et al., “Analysis of nanoindentation load-displacement loading curves” (1996).
- Bec S. et al., “Improvements in the indentation method with a surface force apparatus” (1996).
- Menčík J. et al., “Determination of elastic modulus of thin layers using nanoindentation” (1997).

- Bolshakov A. and Pharr G. M., “Influences of pile-up on the measurement of mechanical properties by load and depth sensing indentation techniques.” (1998).
- Cheng Y.T. and Cheng C.M. ,”Effects of ‘sinking in’ and ‘piling up’ on estimating the contact area under load in indentation.” (1998).
- Cheng Y.T. and Cheng C.M. ,”Relationships between hardness, elastic modulus, and the work of indentation.” (1998).
- Hochstetter G. et al., “Strain-rate effects on hardness of glassy polymers in the nanoscale range. Comparison between quasi-static and continuous stiffness measurements” (1999).
- Malzbender J. and de With G., “Indentation load–displacement curve, plastic deformation, and energy.” (2002).
- Li X. and Bhushan B., “A review of nanoindentation continuous stiffness measurement technique and its applications.” (2002).
- Oliver W.C. and Pharr G.M., “Measurement of hardness and elastic modulus by instrumented indentation: Advances in understanding and refinements to methodology” (2004).
- Cheng Y.T. and Cheng C.M., “Scaling, dimensional analysis, and indentation measurements.” (2004).
- Fischer-Cripps A.C., “Critical review of analysis and interpretation of nanoindentation test data” (2006).
- Guillonneau G. et al.,”Extraction of mechanical properties with second harmonic detection for dynamic nanoindentation testing.” (2012).
- Guillonneau G. et al., “Determination of mechanical properties by nanoindentation independently of indentation depth measurement” (2012).
- Yetna N’jock M. et al., “A criterion to identify sinking-in and piling-up in indentation of materials.” (2015).

Correction factors and Correction of experimental data

- King R.B., “Elastic analysis of some punch problems for a layered medium” (1987).
- Menčík J., “Determination of elastic modulus of thin layers using nanoindentation” (1997).
- Hay J.C. et al., “A critical examination of the fundamental relations used in the analysis of nanoindentation data” (1999).
- Troyon M. and Lafaye S., “About the importance of introducing a correction factor in the Sneddon relationship for nanoindentation measurements” (2002).
- Strader J.H. et al., “An experimental evaluation of the constant b relating the contact stiffness to the contact area in nanoindentation.” (2006).
- Fischer-Cripps A.C., “Critical review of analysis and interpretation of nanoindentation test data” (2006).
- Jakes J.E. et al., “Experimental method to account for structural compliance in nanoindentation measurements” (2008).
- Pharr G.M. et al., “Critical issues in making small-depth mechanical property measurements by nanoindentation with continuous stiffness measurement” (2009).
- Kaufman J. D. and Klapperich C. M., “Surface detection errors cause overestimation of the modulus in nanoindentation on soft materials” (2009).
- Li H. et al., “New methods of analyzing indentation experiments on very thin films” (2010).
- Piccarolo S. et al., “Improving surface detection on nanoindentation of compliant materials” (2010).

Bilayer models to extract Young's modulus of a thin film on a substrate (with conical indenters)

- Bückle H., "VDI Berichte" (1961).
- Doerner M.F. and Nix W.D.,"A method for interpreting the data from depth-sensing indentation instruments" (1986).
- Yu H.Y. et al., "The effect of substrate on the elastic properties of films determined by the indentation test - axisymmetric Boussinesq problem" (1990).
- Pharr G.M. and Oliver W.C., "Measurement of Thin Film Mechanical Properties Using Nanoindentation" (1992).
- Gao H. et al., "Elastic contact versus indentation modeling of multi-layered materials" (1992).
- Menčík J. et al., "Determination of elastic modulus of thin layers using nanoindentation" (1997).
- Chen X. and Vlassak J.J., "Numerical study on the measurement of thin film mechanical properties by means of nanoindentation" (2001).
- Rar A. et al., "Assessment of new relation for the elastic compliance of a film–substrate system." (2002).
- Saha R. and Nix W.D., "Effects of the substrate on the determination of thin film mechanical properties by nanoindentation" (2002).
- Chen S. et al., "Nanoindentation of thin-film-substrate system: Determination of film hardness and Young's modulus" (2004).
- Jung Y.-G. et al. "Evaluation of elastic modulus and hardness of thin films by nanoindentation" (2004).
- Perriot A. and Barthel E., "Elastic contact to a coated half-space: Effective elastic modulus and real penetration" (2004).
- Bec S. et al., "A simple guide to determine elastic properties of films on substrate from nanoindentation experiments" (2006).
- Xu H. and Pharr G.M., "An improved relation for the effective elastic compliance of a film/substrate system during indentation by a flat cylindrical punch." (2006).
- Korsunsky A.M. and Constantinescu A., "The influence of indenter bluntness on the apparent contact stiffness of thin coatings" (2009).
- Li H. and Vlassak J.J., "Determining the elastic modulus and hardness of an ultra-thin film on a substrate using nanoindentation" (2009).
- Sakai M., "Substrate-affected indentation contact parameters of elastoplastic coating/substrate composites" (2009).
- Hay J. and Crawford B., "Measuring substrate-independent modulus of thin films" (2011).
- Bull S.J., "Mechanical response of atomic layer deposition alumina coatings on stiff and compliant substrates" (2011).
- Bull S.J., "A simple method for the assessment of the contact modulus for coated systems." (2014).
- Li Y. et al., "Models for nanoindentation of compliant films on stiff substrates" (2015).

Multilayer models to extract Young's moduli of thin films on a multilayer sample (with conical indenters)

- Pailler-Mattei C. et al., "In vivo measurements of the elastic mechanical properties of human skin by indentation tests" (2008).

- Mercier D. et al., "Young's modulus measurement of a thin film from experimental nanoindentation performed on multilayer systems" (2010).
- Mercier D., "Lois de comportement des matériaux utilisés dans les contacts électriques pour application " flip chip "" (2013).
- Constantinescu A. et al., "Symbolic and numerical solution of the axisymmetric indentation problem for a multilayered elastic coating" (2013).
- Puchi-Cabrera. E.S. et al., "A description of the composite elastic modulus of multilayer coated systems" (2015).

Bilayer models to extract hardness of a thin film on a substrate (with conical indenters)

- Bückle H., "VDI Berichte" (1961).
- Kao P.-W. and Byrne J. G., "Ion Implantation Effects on Fatigue and Surface Hardness" (1981).
- Jönsson B. and Hogmark S., "Hardness measurements of thin films" (1984).
- Doerner M.F. et al., "Plastic properties of thin films on substrates as measured by submicron indentation hardness and substrate curvature techniques" (1986).
- Burnett P.J. and Rickerby D.S., "The mechanical properties of wear-resistant coatings: I: Modelling of hardness behaviour." (1987).
- Burnett P.J. and Rickerby D.S., "The mechanical properties of wear-resistant coatings: II: Experimental studies and interpretation of hardness." (1987).
- Page T.F. et al., "Nanoindentation Characterisation of Coated Systems: P:S2 - A New Approach Using the Continuous Stiffness Technique" (1998).
- Fernandes J.V. et al., "A model for coated surface hardness" (2000).
- Han S.M. et al., "Combinatorial studies of mechanical properties of Ti–Al thin films using nanoindentation" (2005).
- Han S.M. et al., "Determining hardness of thin films in elastically mismatched film-on-substrate systems using nanoindentation" (2006).

Multilayer models to extract hardness of thin films on a multilayer sample (with conical indenters)

- Engel P.A. et al., "Interpretation of superficial hardness for multilayer platings*" (1992).
- Rahmoun K. et al., "A multilayer model for describing hardness variations of aged porous silicon low-dielectric-constant thin films" (2009).
- Arrazat B. et al., "Nano indentation de couches dures ultra minces de ruthénium sur or" (2010).

Finite Element Modelling of conical indentation of thin film(s) on a substrate

- Charleux L., "Abapy Documentation"
- ABAQUS documentation
- Bhattacharya A.K. and Nix W.D., "Finite element analysis of cone indentation." (1991).
- Madsen D.T. et al. "Finite Element Simulation of Indentation Behavior of thin Films." (1991).
- Sun Y. et al., "Finite element analysis of the critical ratio of coating thickness to indentation depth for coating property measurements by nanoindentation." (1995).

- Hubert N. et al. “Identification of elastic-plastic material parameters from pyramidal indentation of thin films.” (2002).
- He J.L. and Veprek S., “Finite element modeling of indentation into superhard coatings.” (2003).
- Cai X. and Bangert H., “Hardness measurements of thin films-determining the critical ratio of depth to thickness using FEM.” (2005).
- Bolshakov A. and Pharr G.M., “Influences of pile-up on the measurement of mechanical properties by load and depth sensing indentation techniques.” (1998)
- Lichinchi M. et al., “Simulation of Berkovich nanoindentation experiments on thin films using finite element method.” (1998).
- Chen X. and Vlassak J.J., “A Finite Element Study on the Nanoindentation of Thin Films.” (2000).
- Chen X. and Vlassak J.J., “Numerical study on the measurement of thin film mechanical properties by means of nanoindentation.” (2001).
- Bouzakis K.-D. et al., “Thin hard coatings stress–strain curve determination through a FEM supported evaluation of nanoindentation test results.”, (2001).
- Xu Z.-H. and Rowcliffe D., “Finite element analysis of substrate effects on indentation behaviour of thin films.” (2004).
- Panich N. and Sun Y. “Effect of penetration depth on indentation response of soft coatings on hard substrates: a finite element analysis” (2004)
- Bressan J.D. et al., “Modeling of nanoindentation of bulk and thin film by finite element method.” (2005).
- Pelletier H. et al., “Characterization of mechanical properties of thin films using nanoindentation test.” (2006)
- Xu H., “A Finite Element Study of the Contact Stiffness of Homogenous Materials and Thin Films.” PhD thesis - University of Tennessee - Knoxville (2007)
- Antunes J.M. et al., “On the determination of the Young’s modulus of thin films using indentation tests” (2007).
- Chen S.H. et al., “Small scale, grain size and substrate effects in nano-indentation experiment of film–substrate systems.” (2007).
- Huang X. and Pelegri A.A., “Finite element analysis on nanoindentation with friction contact at the film/substrate interface.” (2007).
- Pelegri A.A. and Huang X., “Nanoindentation on soft film/hard substrate and hard film/soft substrate material systems with finite element analysis.” (2008).
- Wittler O. et al., “Mechanical characterisation of thin metal layers by modelling of the nanoindentation experiment.” (2008).
- Sakharova N.A. et al., “Comparison between Berkovich, Vickers and conical indentation tests: A three-dimensional numerical simulation study.” (2009).
- Chen C., “2-D Finite Element Modeling for Nanoindentation and Fracture Stress Analysis.” PhD thesis - University of South Florida (2009).
- Moore S.W. et al., “Nanoindentation in elastoplastic materials: insights from numerical simulations.” (2010).
- Dowhan L. et al., “Investigation of thin films by nanoindentation with doe and numerical methods.” (2011).
- Isselé H. et al., “Determination of the Young’s modulus of a TiN Thin Film by nanoindentation: analytical models and numerical FEM simulation.” (2012).
- Phiciato’s blog (2013)
- Moćko W. et al., “Simulation of nanoindentation experiments of single-layer and double-layer thin films using finite element method.” (2014).

- Kibech S. et al., “Nanoindentation” (2014).
- Kopernik M. and Milenin A., “Numerical modeling of substrate effect on determination of elastic and plastic properties of TiN nanocoating in nanoindentation test.” (2014).
- Li Y. et al., “Models for nanoindentation of compliant films on stiff substrates” (2015).
- Gupta A. K. et al., “Evaluation of elasto-plastic properties of ITO film using combined nanoindentation and finite element approach” (2015).

1.7.4 Softwares

- IndentAnalyser by ASMEC
- Elastica by ASMEC
- Softwares from SIOMEC
- Softwares from Keysight
- Piuma dataviewer
- Punias
- Gwyddion
- Softwares from Nanovea
- Virtual nanoindenter
- Nanoindentation from Kibech S. et al.

1.7.5 Reviews / Overviews of nanoindentation technique

- Li X. and Bhushan B., “A review of nanoindentation continuous stiffness measurement technique and its applications.” (2002).
- VanLandingham M.R., “Review of Instrumented Indentation” (2003).
- Fischer-Cripps A.C., “Nanoindentation” Springer 3rd Ed. (2011).
- Oliver W.C. and Pharr G.M., “Measurement of hardness and elastic modulus by instrumented indentation: Advances in understanding and refinements to methodology” (2004).
- Fischer-Cripps A.C., “Critical review of analysis and interpretation of nanoindentation test data” (2006).
- Lucca D.A. et al., “Nanoindentation: Measuring methods and applications” (2012).
- Němeček J., “Nanoindentation in Material Science” (2012).
- Michailidis N. et al., “Nanoindentation” (2014).

1.7.6 Reviews / Overviews of nanoindentation technique applied to coatings

- Pharr G.M. and Oliver W.C., “Measurement of Thin Film Mechanical Properties Using Nanoindentation” (1992).
- Mencík J. et al., “Determination of elastic modulus of thin layers using nanoindentation” (1997).
- Nix W.D., “Elastic and plastic properties of thin films on substrates: nanoindentation techniques” (1997).

- Van Vliet K.J. and Gouldstone A., "Mechanical Properties of Thin Films Quantified Via Instrumented Indentation" (2001).
- Fischer-Cripps A.C., "Nanoindentation" Springer 3rd Ed. (2011).
- Šimůnková Š., "Mechanical properties of thin film–substrate systems" (2003).
- Bull S.J., "Nanoindentation of coatings" (2005).

1.7.7 Books

- Johnson K.L., "Contact Mechanics" (1987), ISBN - 9780521347969.
- Bhushan B., "Micro/Nanotribology and Its Applications" (1997).
- Fischer-Cripps A.C., "Introduction to Contact Mechanics" Springer 1st Ed. (2000).
- Fischer-Cripps A.C., "Nanoindentation" Springer 1st Ed. (2002).
- Fischer-Cripps A.C., "Nanoindentation" Springer 2nd Ed. (2004).
- Fischer-Cripps A.C., "Introduction to Contact Mechanics" Springer 2nd Ed. (2007).
- Fischer-Cripps A.C., "Nanoindentation" Springer 3rd Ed. (2011).
- Tiwari A., "Nanomechanical Analysis of High Performance Materials" Springer Vol. 203 (2014).

CHAPTER 2

Contact

Author David Mercier [1]

[1] Max-Planck-Institut für Eisenforschung, 40237 Düsseldorf, Germany

CHAPTER 3

Acknowledgements

The author is grateful to Dr. V. Mandrillon from (CEA, France (Grenoble)) and to Dr. M. Verdier from (SIMaP, France (Grenoble)), for long discussions and many advices about nanoindentation.

The author is grateful to Dr. Igor Zlotnikov (Max Planck Institute of Colloids and Interfaces, Germany (Potsdam)), for providing example files.

CHAPTER 4

Keywords

Matlab toolbox ; nanoindentation ; conical indenter ; Young's modulus ; hardness ; thin film ; multilayer system ; analytical model ; python script ; finite element modelling.